University of Nevada, Reno

A Unique Instrumentation System Design for Measuring Forces on a Rotating Shaft

A thesis submitted in partial fulfillment of the requirements for the degree of Master of Science with a major in Computer Engineering

by

John R. Kearney

Dr. Frederick C. Harris, Jr., Thesis Advisor

May, 2008

THE GRADUATE SCHOOL

We recommend that the thesis
prepared under our supervision by

JOHN R. KEARNEY

entitled

**A Unique Instrumentation System Design
for Measuring Forces on a Rotating Shaft**

be accepted in partial fulfillment of the
requirements for the degree of

MASTER OF SCIENCE

Frederick C. Harris Jr., Ph.D., Advisor, Committee Chair

Dwight Egbert, Committee Member

James Henson, Ph.D., Graduate School Representative

Marsha H. Read, Ph.D., Associate Dean, Graduate School

May, 2008

Abstract

The design and construction of instrumentation systems require a broad background in many disciplines. The system design in this thesis was further complicated by the subject of the measurement. Attempting to measure the bending forces on a rotating shaft is difficult in the extreme. I believe that the approach taken in the design of this Instrumentation and Measurement System is unique and has broader applications than that described by this thesis. There is significant opportunity to further the performance of the Instrumentation and Measurement system as well as the post processing analysis tools.

Dedication

To first and foremost, my wife Jean who read and corrected much of the grammar and spelling of what you read here, to Dr. John Kleppe who first encouraged me to enter the Master's program and made possible my first year of Graduate School and finally to Dr. Bruce Johnson who kept after me for over 20 years to get my undergraduate degree.

Acknowledgments

First, I would like to recognize the help, support and direction received from Dr. Frederick Harris in the completion of this thesis. Several professors during the course of my graduate studies have provided knowledge, insight and support and I wish to thank them all. I would like to give special thanks to the members of my committee, Professor Dwight Egbert, Computer Engineering and Dr. James Henson, Electrical Engineering. Their classes provided most of the reference and source material for this thesis.

Outside of school, many individuals from the Corvair Aircraft Engine community contributed to the information contained in this thesis, but three were essential contributors to the basic design as well as testing the system. The first is Mark Langford from Huntsville, AL. Mark has survived three in-flight crank shaft failures. He has collected and documented most of the engineering research on the subject. The second is Dan Benson of PRS Engineering. Dan and some of his staff performed the solid modeling and the metallurgy research referenced in the document. The third is Mr. William Wynne, my Corvair mentor and foremost proponent of the Corvair Aircraft Engine Conversion. In essence, William wrote and is still writing the book on this conversion.

In addition, I would also like to express my appreciation to Fred and Al Gangi of Newest computers Inc., Reno Nevada for the layout and manufacturing of the accelerometer sensor boards used in this project; to Hodges Transportation Inc., Silver Springs NV for calibration of the accelerometers, and to Mr. Rick Capps for his support and encouragement.

Contents

List of Figures

List of Tables

Chapter 1 Introduction

Instrumentation is a critical element for control systems and a design validation tool. In this latter role, instrumentation may also be utilized to perform measurements on systems that are utilized in applications for which they were not initially designed. It is these systems that present the greatest challenges to the design and use of instrumentation systems.

A prime example is automotive engines used in experimental recreational aviation. The use of automotive engines in aircraft is driven by purely financial considerations. An automotive engine converted for aircraft use is approximately one-third the cost of a certified aircraft engine. These conversions often exhibit systemic problems or failures whose cause is difficult to determine. In this situation instrumentation systems are the primary tools used to isolate and identify the root cause or causes of the system failures.

Crankshaft failure in these conversions presents the most difficulty. This thesis describes the development and evaluation of an instrumentation and measurement system designed to identify the root cause of crankshaft failures. Crankshafts fail as a result of excessive force or fatigue due to repetitive bending moments. The problem presented to the instrumentation engineer is how to measure forces on a rotating body.

Instrumentation systems typically consist of three major components; sensors, signal conditioning components and data recorders. The instrumentation design described here introduces a unique approach to measuring the physical forces on the shaft by applying the principals of Newtonian physics - specifically Newton's three laws of motion. The usual method of measuring bending moments is direct measurement of the bending forces by measuring the bending moment of the metal itself.

The rest of this thesis will demonstrate that bending forces can be determined with reasonable accuracy by taking advantage of these principals and designing custom sensors. In addition, once the data have been gathered, it is necessary to analyze them to isolate and identify the root cause of the failures. To implement this design and to perform the analysis requires the application of three major engineering disciplines: Electrical Engineering, Computer Science and Mechanical Engineering, along with the fundamental foundations provided by physics and mathematics.

This thesis is structured as follows: Chapter 2 provides the basic information on instrumentation systems including sensors, signal conditioning components and recording devices. Chapter 3 describes the overall requirements including information on the operation of reciprocating engines, a short discussion on the forces placed on an aircraft, the project plan as implemented including an overview of the system components, processes and tools used to design and build the instrumentation and measurement system. Chapters 4 and 5 describes the actual hardware design and the software designs respectively, and Chapter 6 shows the results of the project including preliminary data analysis. Chapter 7 outlines the future work to be performed on the project.

Chapter 2 Background

2.1 Instrumentation and Measurement

> "*A very common feeling about measurement activity is that it does not involve anything else than connecting a suitable instrument to a measured system, reading the instrument's display and, if needed, making a few calculations on the value provided by the instrument*." [1]

While this approach is most often used, it may not accomplish the overall objective. As Dr. Alessandro Ferrero, Politecnico di Milano, Italy, and Dr. Dario Petri, University of Trento, Italy, state in their syllabus for advanced studies in instrumentation and measurement:

> "*there is a "but" that motivates this School: the old question, debated by Socrates, about the role of the empirical knowledge, and the old question, already asked at Augustus time, about how well the measurement result describes the measured, are still open questions and the evolution of the modern instruments only makes them more difficult to answer".*
>
> *"… finding an answer to the second question is the task of the science of measurement and measurement engineers. To accomplish this task, the knowledge of the instruments and their operating principles is important, but it is not enough. A solid background about the fundamentals of the measurement science, the measurement methods, the mathematical basis of either signal analysis and digital signal processing, the mathematical theories for representing incomplete knowledge and the current Standards is required."* [1]

It is this understanding of principals that enables us to design instrumentation and measurement systems that perform measurements on our target system, and to determine how close the measurement is to the actual performance of the item measured. The closer we can come to bringing these two issues into equality, the better the description we will have of the measured system, which is, after all, what we are trying to achieve.

2.2 Components of an Instrumentation and Measurement System

A typical instrumentation system consists of three major classes of components: sensors, signal conditioners and the data recorder. Here we discuss the primary sensor technologies that are applicable to this project, the reason for and methods of signal conditioning, and, finally, the different types of recording methods.

The goal of our instrumentation system is to detect bending moments on a rotating shaft. Although many sensors are used in instrumentation and measurement systems, this paper focuses on the sensors that were considered for this design. To understand the tradeoffs we evaluated, a basic understanding of these sensors is necessary. Section 2.2.1 provides basic understanding and may be skipped by those experienced with the theory and application of sensors, signal conditioners and recording devices.

2.2.1 Sensors

2.2.1.1 Strain Gauges

The principal sensor used to measure the bending moment in a rigid structure is the strain gauge. A strain gauge is a metal foil device attached to the structure subject to the bending forces. Figure 2.1 shows an example.

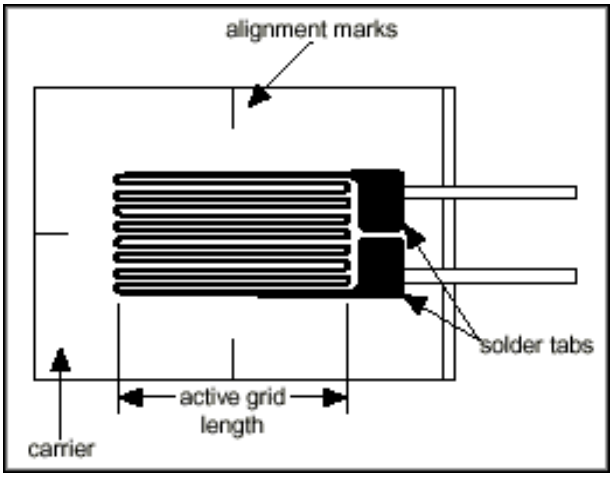

Figure 2.1 Strain Gauge [2]

The electrical resistance of the device varies as it is deformed or bent. It measures very slight bending distances and tolerates a deflection that is typically less than 1mm across the direction of sensitivity for steel structures. If the gauge is deflected more than the allowed distance, the gauge will fail to an-out-of range value and will have to be replaced. Temperature also affects strain gauge operation. As the metal expands and contracts due to temperature change, the output of the sensor changes significantly. To combat this problem a second gauge is used, oriented in a plane perpendicular to the forces that are being measured, as shown in Figure 2.2. This has the effect of canceling the variations due to temperature as both gauges will be affected equally and the second gauge's output can be subtracted from the primary measurement gauge.

This “half bridge” sensor configuration is utilized when single direction force is of interest.

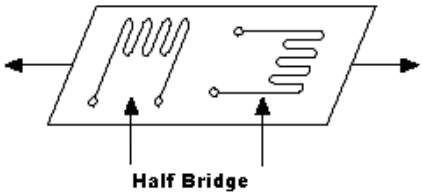

Figure 2.2 Half Bridge

This configuration is called a “half bridge” due more to the way it is connected to the signal conditioning system, than to its placement. Even though the gauges shown in this illustration are side by side, the gauges are placed on top of each other when installed. A common electronic circuit used to detect small changes in resistance is the resistive bridge circuit or “Wheatstone Bridge”. An example circuit is shown in Figure 2.3.

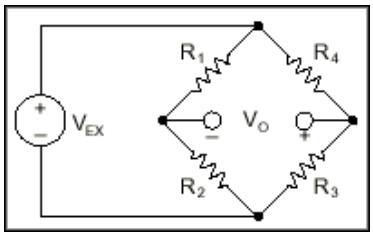

Figure 2.3 Resistive (Wheatstone) Bridge Circuit [2]

The resistors are selected with high precision to match the DC resistance of the sensor. The basic theory is that if all of the resistances are equal, the voltage potential between the V_o terminals will be equal to 0 volts. The strain sensor typically replaces R3, R4 or both depending on the application. For the half bridge application, the two

gauges shown in Figure 1 replace both R3 and R4. This results in the circuit shown in Figure 2.4.

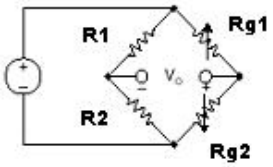

Figure 2.4 Half Bridge Strain Gauge Circuit

In this configuration, the perpendicular gauge acts to remove the measurement variations caused by the expansion and contraction of the metal caused by changes in temperature. The part of the signal that remains is a measure of the force acting on the metal. To measure the forces in more than one direction, strain gauges can be purchased in clusters or "rose buds" which provide up to three gauges oriented 60^{o} and provide the ability to determine force vectors in addition to simple magnitude. These gauges are usually connected to two full bridge circuits as shown in Figure 2.5.

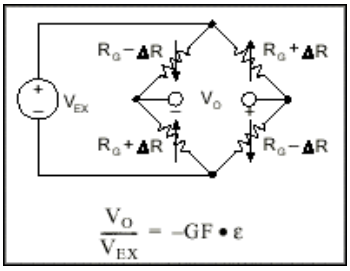

Figure 2.5 Full Bridge Strain Gauge Circuit [2]

A final note about the installation of strain gauges; these sensors are very fragile and break easily. They require the services of a skilled technician to install and are not

robust. They are typically used in very controlled environments where their performance can be predicted and are not utilized for extended periods of time.

Although different types of strain gauges are used in everything from load cells to pressure transducers, the only way to use them to measure the force in a rigid body is to install them directly on a spotless part of the metal structure.

2.2.1.2 Accelerometers

The following excerpt from National Instruments web site describes the fundamental principal of an accelerometer: [3]

> *"Newton's law simply states that if a mass,* **m***, is undergoing an acceleration,* **a***, then there must be a force* **F** *acting on the mass and given by* **F = ma***. Hooke's law states that if a spring of spring constant* **k** *is stretched (extended) from its equilibrium position for a distance* **Dx,** *then there must be a force acting on the spring given by* **F** = **kDx***.*

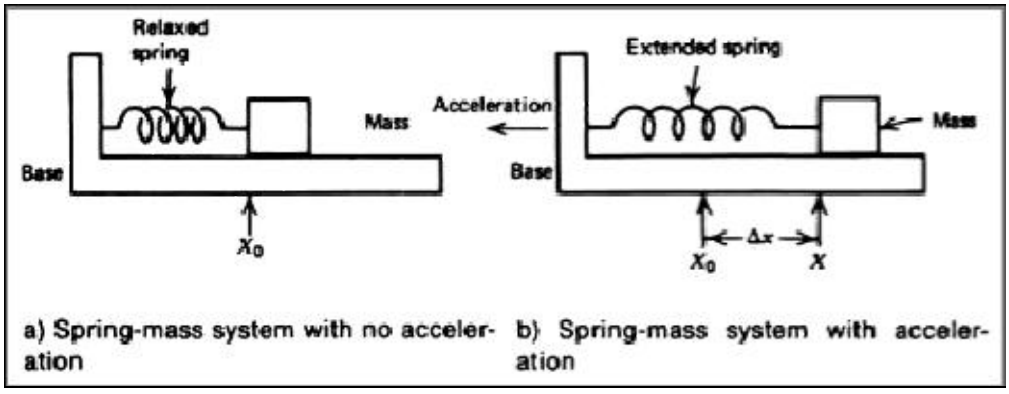

FIGURE 5.23 The basic spring-mass system accelerometer.

> *In Figure 5.23a we have a mass that is free to slide on a base. The mass is connected to the base by a spring that is in its unextended state and exerts no force on the mass. In Figure 5.23b, the whole assembly is accelerated to the left, as shown. Now the spring extends in order to provide*

the force necessary to accelerate the mass. This condition is described by equating Newton's and Hooke's laws:

ma = **kDx** ***(5.25)***

where **k** = *spring constant in* **N/m**
Dx = *spring extension in m*
m = *mass in kg*
a = *acceleration in m/s*^{2}

Equation (5.25) allows the measurement of acceleration to be reduced to a measurement of spring extension (linear displacement) because

$$a = \frac{k}{m}\Delta x \qquad (5.26)$$

If the acceleration is reversed, the same physical argument would apply, except that the spring is compressed instead of extended. Equation (5.26) still describes the relationship between spring displacement and acceleration.

The spring-mass principle applies to many common accelerometer designs. The mass that converts the acceleration to spring displacement is referred to as the test mass or seismic mass. We see, then, that acceleration measurement reduces to linear displacement measurement; most designs differ in how this displacement measurement is made."

One of the drawbacks of spring mass accelerometer sensors is that they have an ultimate yield point. This fact presents a problem to the designer of an instrumentation system: the higher the yield point of the sensor, the less sensitive the device. Most modern day accelerometers have some type of mass beam on a piezo resistive or piezo capacitive material. The materials these devices are made of have an ultimate yield point that must be taken into consideration. If there is a need for high sensitivity and the ability to withstand large shock loads and continue to operate, then a different technology is required.

Figure 2.6 describes an alternative accelerometer that uses a thermal bubble encapsulated within a structure and a thermal grid to measure acceleration. This device can withstand the high shock loads and provide good sensitivity.

> *"Temperature sensors equidistant from the heater measure the same temperature until device is accelerated as shown in bottom picture. Acceleration of the sensor creates a non-symmetrical temperature profile from which acceleration is detected as shown in the top picture."*[4]

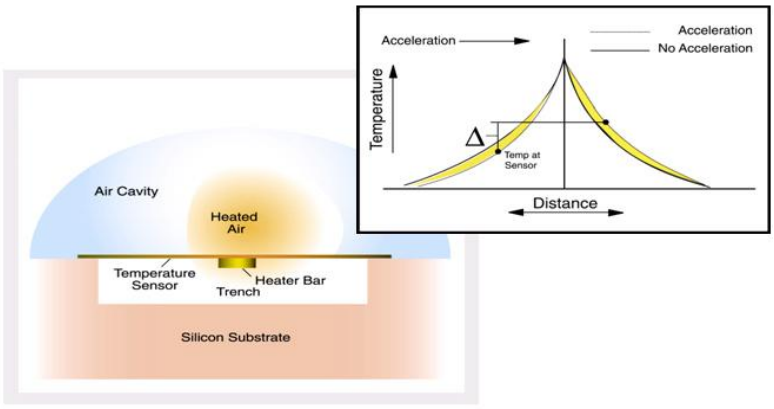

Figure 2.6 Thermal Accelerometer Design [4]

Because this type of device has no mass beam-sensing element and depends only on the thermal "bubble", it can survive shock loads, and when the shock load is removed, the accelerometer is able to return back to its primary sensitivity.

2.2.1.3 Inductive Pickups

The final sensor that we will cover is a simple inductive pickup. Its purpose is to detect current flow or, alternatively, a change in current flow. This is accomplished by winding the sensor wire around a primary current carrying wire. The magnetic field created by the current flowing in the wire induces a smaller current in the sensor winding. We convert this current to a voltage across a resistor, and we then measure

that voltage. The application of this sensor is described in the Chapter 4, Instrumentation and Measurement System design. A basic characteristic of this sensor is that the inductive pickup is a differential sensor that relies on a change in current in the primary wire to induce a current in the sensor wiring.

2.2.2 Signal Conditioners

> *"Signal conditioners are measuring system elements that start with an electric sensor output and then yield a signal suitable for transmission, display or recording, or that better meet the requirements of a subsequent standard equipment or device."*[5]

In other words, signal conditioning circuits are designed to provide level shifting, gain and filtering for each sensor node in the system. Each of the sensors described requires a different type of signal conditioning.

2.2.2.1 Resistive Sensor Signal Conditioning

The Wheatstone Bridge shown in Figure 2.7 (electrically the same as in Figure 2.3) uses resistors of the same value to create a set of parallel voltage dividers:

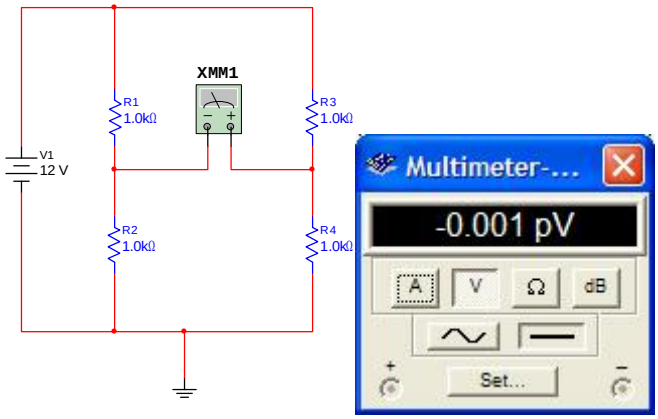

Figure 2.7 Wheatstone Bridge Equivalent and Meter [6]

As can be seen on the meter's display, a balanced bridge has a small differential voltage between the resistors in the center of the bridge, showing here as –0.001pico volts or $1x10^{-15}$ volts. Figure 2.8 shows what happens when a "half bridge" sensor replaces R3 and R4.

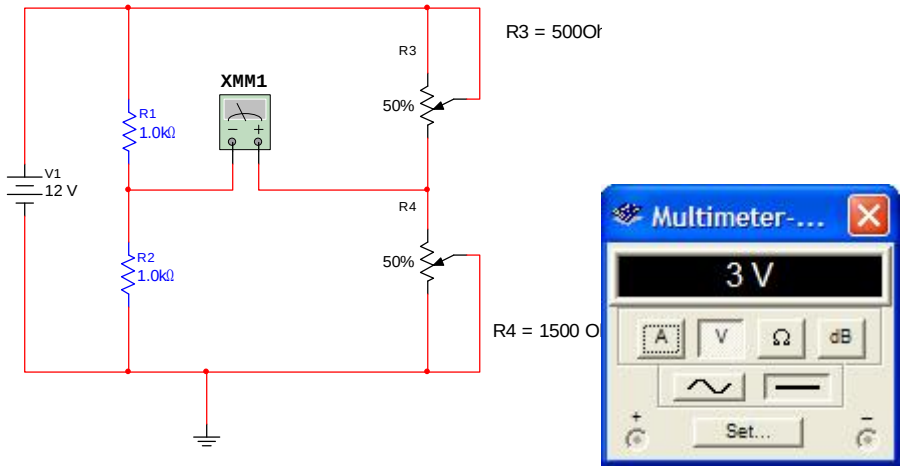

Figure 2.8 Unbalanced Wheatstone Bridge with Meter [6]

In this case, the resistances for each individual sensor move in opposite directions. R3 decreases resistance by 500 Ohms and R4 increases resistance by 500 Ohms, resulting in a significant change in the differential voltage in the center of the bridge. This illustration is exaggerated for the purpose of explanation. Normally, strain sensors would change only a few Ohms, and the difference voltage for full deflection would not be as large. Typical resistance values for strain gauges are 350 Ohms with a variance of +/- 5 to 7 Ohms. Using the following formula we can determine the maximum voltage change from a typical half bridge circuit:

$V_o = V_s\left(\frac{R_3}{R_3+R_4} - \frac{R_2}{R_2+R_1}\right)$ where R_1 and R_2 are 350 Ohms, the second half of the equation results in ½.V_s. We will use Vs of 10 Volts for our example to make computation easier. This means that the R1 R2 junction will be 10 Volts * ½ = 5 Volts. This is the reference side of our bridge. Now we will compute the sensor side assuming a maximum deflection toward R3 from the normal position. Assuming that the maximum resistance variation is 5 Ohms over the distance we obtain the following formula:

$$V_o = V_s\left(\frac{R_3}{R_3+R_4}\right) - 5V = 10V\left(\frac{355\Omega}{355\Omega+345\Omega}\right) - 5V$$
$$= 10V\left(\frac{355\Omega}{700\Omega}\right) - 5V = 5.071V - 5V = 0.071\,V$$

Now if we assume that a full deflection in the opposite direction will result in the same value with opposite polarity (*i.e. –0.071V*), we get a maximum difference voltage from full negative to full positive of 0.142 V with a zero point offset of 0.71V. This is below the normal sensitivity of analog-to-digital converters, therefore, it is necessary to amplify the signal into a range that can be used by the recorder.

Analog-to-digital converters (ADC) operate at many voltage ranges, but for our purpose let us assume that we have a 0 to 5 volts ideal ADC (*Ideal ADCs have completely linear response from the two power rails*). If we want to approach the full scale capabilities of our ADC, we need to make our 0.142 V differential voltage appear to the ADC as 0 to 5V. This requires a gain of about 35, so we need to amplify the signal 35 times to approach the 5 V range of our ADC.

Now, however, we have a problem. If we want to have the center point of our gauge to be at the center point of our ADC, we need to offset the signal from the Wheatstone bridge. The center point of the Wheatstone bridge is essentially 0 when there is no bending or strain on the gauges. If we try to use a resistance on the output of the bridge, we will change both the performance and linearity of the circuit, defeating its primary purpose. This problem is solved by the differential instrumentation amplifier. This device has extremely high input impedance with the ability to produce large gains, and it meets the requirements for our ADC.

2.2.2.2 Instrumentation Amplifiers

An instrumentation amplifier is a specific type of operational amplifier. Although these devices come in a package indicating a single amplifier as shown in Figure 2.9, they are actually made up of several amplifiers in a specific configuration.

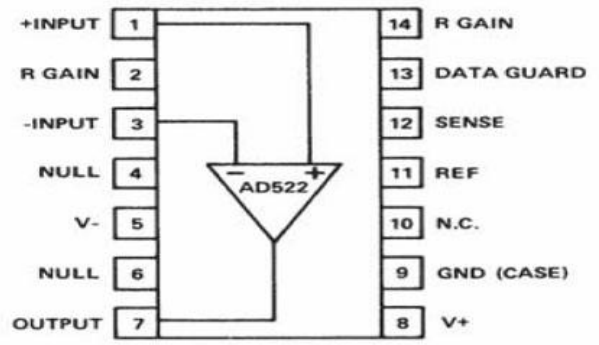

Figure 2.9 AD522 Differential Amplifier [7]

The device is internally configured as shown in Figure 2.10.

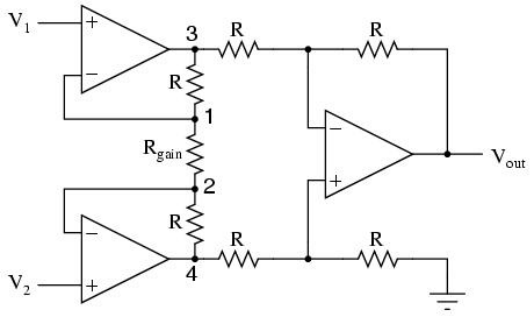

Figure 2.10 Internal Design of Differential Amplifier [8]

This type of configuration provides several advantages over single-ended amplifiers in that they provide low DC offset, low drift, large open loop gain, high input impedances, excellent common mode rejection, great stability and accuracy.

These devices are best used on sensors like the strain gauge where placing a low resistance across the terminals will significantly change the response of the Wheatstone bridge as shown in Figure 2.11.

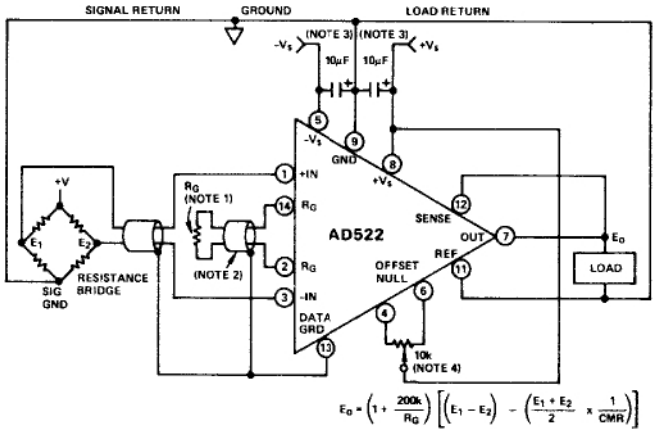

Figure 2.11 Example Differential Amplifier Connected to Wheatstone Bridge [7]

Due to their high accuracy, stability and gain, these devices are also used on active circuits to provide filtering and additional scaling. Connecting the +IN terminal to ground

and using the amplifier in the normal way as shown in Figure 2.12 will modify the gain of this device.

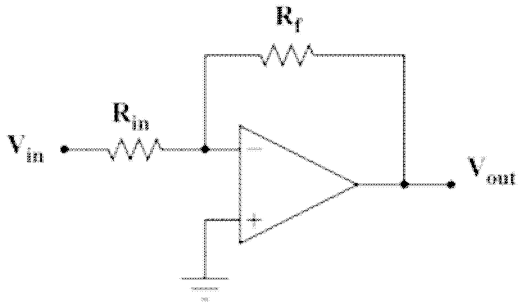

Figure 2.12 Differential Amplifier in Single Ended Inverting Configuration [9]

2.2.2.3 Reactive Sensor Signal Conditioning

The last instrumentation amplifier configuration that we will evaluate in our design is the comparator. This device provides a rail-to-rail change in output if the input falls above or below the reference value. Figure 2.13 shows the circuit for using an operational amplifier as a comparator.

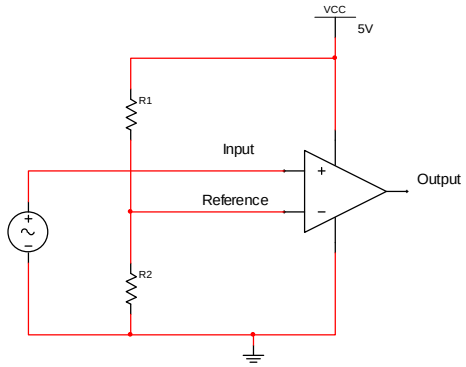

Figure 2.13 Differential Amplifier as a Comparator

In this configuration the output will go to the positive rail, 5 volts in this case, when the input value is above 2.5 volts, assuming that R1 and R2 are equal, and will be at the

negative rail, ground in this case, when the input value is below 2.5 volts. This circuit is used to provide a rail-to-rail square wave that is representative of the AC signal from the inductive pickup.

2.2.2.4 Filters

The final stage of signal conditioning is to filter the input data such that unwanted signals are removed from the data. Filters operate primarily on time varying signals. Filters removed unwanted signals that fall outside of their designed band pass range. Examples are low pass, high pass and band pass.

A low pass filter is utilized when a signal from DC to a specified frequency is desired. This upper frequency is known as the cutoff frequency and is the point at which the filter has reduced the input by 50% or –3 dB. The low pass filter preserves the DC component of the signal and is useful for the absolute accelerometers. The DC component in this case represents the force of gravity on the item to be tested.

The opposite of the low pass filter is the high pass filter. It completely removes the DC component and any frequency lower than its cut off frequency, but does not filter frequencies higher than the cutoff frequency.

The final filter is the band pass filter. This filter combines both a low pass and a high pass filter to pass a range of frequencies. The low pass cutoff is set to a higher frequency than the high pass filter, creating a range of pass band frequencies that are passed through the circuit with minimal alteration to their magnitude. Phase shifts are a side effect of these filters; however, if the phase shifts are kept equal on all channels, the

inter-channel correlation will remain constant with the input signal. This is a critical subject and a major consideration in the design of instrumentation and measurement signal conditioning. The following are example circuits for low pass (Figure 2.14), high pass (Figure 2.15) and band pass (Figure 2.16) filters. Note that these are example circuits and not necessarily those used in our system.

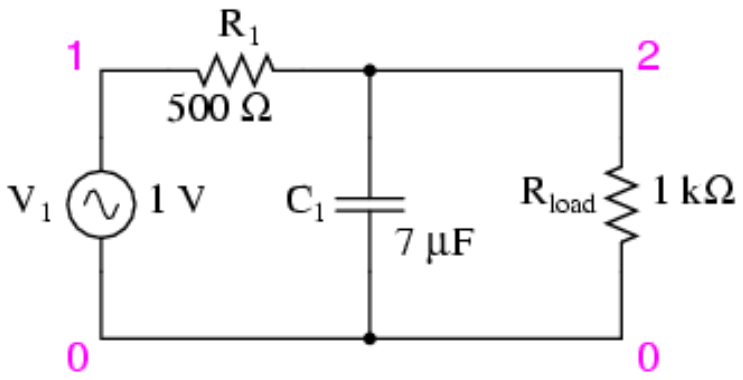

Figure 2.14 Low Pass Filter [10]

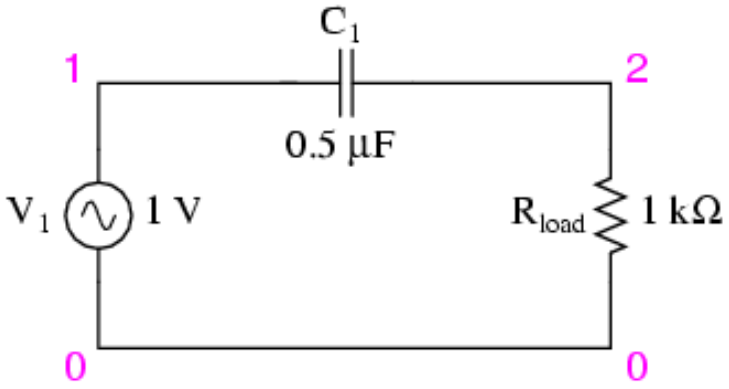

Figure 2.15 High Pass Filter [11]

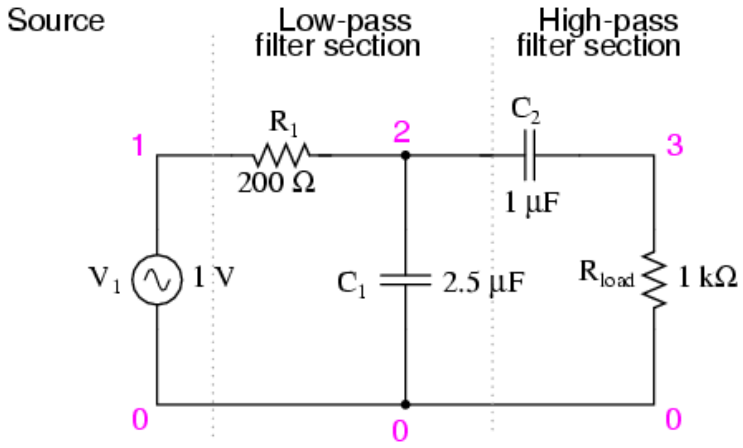

Figure 2.16 Band Pass Filter [12]

2.2.2.5 Analog-to-Digital Converters

Analog-to-digital converters convert an instantaneous voltage to a digital representation of its magnitude. The converter with which we are interested for this application is the flash analog-to-digital converter. Figure 2.17 provides an excellent visualization and description.

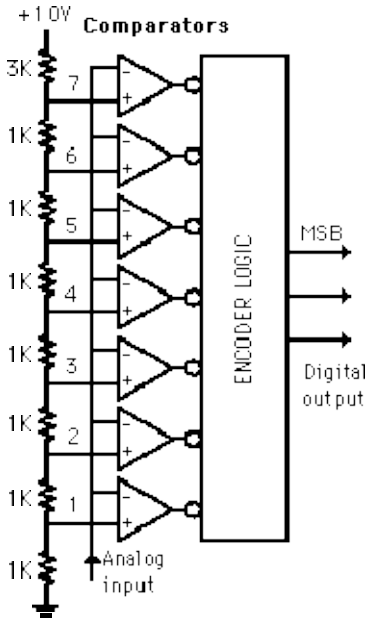

Flash ADC

Illustrated is a 3-bit flash ADC with a resolution of 1 volt. The resistor net and comparators provide an input to the combinational logic circuit, so the conversion time is just the propagation delay through the network - it is not limited by the clock rate or some convergence sequence. It is the fastest type of ADC available, but requires a comparator for each value of output (63 for 6-bit, 255 for 8-bit, etc.) Such ADCs are available in IC form up to 8-bit and 10-bit flash ADCs (1023 comparators) are planned. The encoder logic executes a truth table to convert the ladder of inputs to the binary number output.

Figure 2.17 Flash Analog-to-Digital Converter [13]

Although Figure 2.17 indicates that the maximum bit resolution is 10 bits, there are actually 12-bit, 14-bit and 16-bit ADCs available. Each resolution costs significantly more than the lower resolution devices.

The resolution and the degree of accuracy necessary for the measurement is a critical component of the design process. It can cost too much in both money and time to process highly detailed and accurate data when a lesser resolution and less data can provide the same information. Conversely, if too little resolution or too little information is available, it may be necessary to repeat the tests. Even if the event is transitory, it may be missed altogether and require additional effort to be expended looking for other causes that were just missed in the initial tests. Clearly, a through understanding of the need and purpose of the instrumentation task is the first and most important criteria of the project when designing an instrumentation and measurement system.

2.2.3 Recorders

Since the early days of measurement, recording information has been the most critical step in the process of collecting data. Inaccuracies can occur if the recording system has less resolution than necessary. For example, if you use a tape measure that is graded only in ½ inch increments and you need a length of some material that is 2 $^{5}/_{8}$ inches, the best you can do is to estimate through interpolation. This is the same thing that occurs if a system tries to determine a value between its resolution ranges.

In the digital world, the system will either round up to the next higher value (comparator), round down (inverse comparator) or round near (comparator set at ½ resolution points). The approximation comes only after many samples are taken, and the

result can be weighted by the ratio of numbers larger than the threshold to the numbers lower than the threshold.

Over the years, many methods have been used to record data. Recording devices have included hand written charts, analog strip charts (see Attachment 1, Sensor Calibration Sheets), tape recorders and finally digital recording using computers and other types of digitizing recorders. A full description of these devices is beyond the scope of this thesis; however, any good recording system should provide these basic features:

- Accurate time sequencing for samples,
- Wide enough binary data size to contain the raw data in a single element,
- Digitizing fast enough to provide continuous recording at the desired sample rate,
- Enough storage to provide contiguous data records for a given test, and
- Easy access to retrieve the data.

Although this is not a comprehensive list, it is complete enough for one to understand the issues relating to recording devices. In the next chapter we will examine in greater detail the choices for the project and define the general requirements for this instrumentation and measurement system.

Chapter 3 Instrumentation and Measurement System Design

Accomplishing our task begins with understanding its requirements. Here we define the problem, which determines the requirements of the instrumentation and measurement system needed.

3.1 Problem Background

In experimental aviation, the builder can use any type of engine desired to power their aircraft. A certified aircraft engine can cost as much as the rest of the aircraft combined. To help lower the cost of flying, builders often use automotive engines in their experimental aircraft. However, installing these engines on aircraft can create problems because the engine is used in an application for which it was not intended.

This project was initiated by just such a problem. Since 1964, General Motors Corvair automotive engines have been converted for aircraft use due to their similarity to aircraft engines. Specifically, they are horizontally opposed six-cylinder engines that can produce 100 to 120 horsepower in a direct drive configuration. In the conversion process these engines are rebuilt using new or remanufactured parts to create essentially a new or “zero time” engine. The engine is modified to drive a propeller directly off the crankshaft. This can cause a problem in that the crankshaft bearings in the transmission must now withstand forces that they were not designed to take. When these conversions were first performed, the engine was put on “low and slow” aircraft

that typically flew at airspeeds from 50 mph to 100 mph. Now these engines are in aircraft that are cruising at 150 mph with top speeds exceeding 180 mph.

It is these aircraft that have experienced broken crankshafts in 2005 and 2006. There has been a significant amount of speculation within the conversion community on the cause of the failures, and some engineering analysis has been done. However, the general consensus is that the problem must be caused by one of four specific forces that act on the crankshaft.

3.2 Forces acting on a aircraft crankshaft

Four different propeller forces act on an aircraft engine and specifically the crankshaft. They include P-Factor, gyroscopic, torsional and maneuvering. P-Factor is Illustrated in Figure 3.1 and is defined as:

> *"This effect is seen when the aircraft is moving relatively slowly at a high angle of attack, as in a climb or in slow flight. The descending blade of the propeller meets the oncoming air at a greater angle of attack than the ascending blade creating more thrust on the side of the descending blade."*[14]

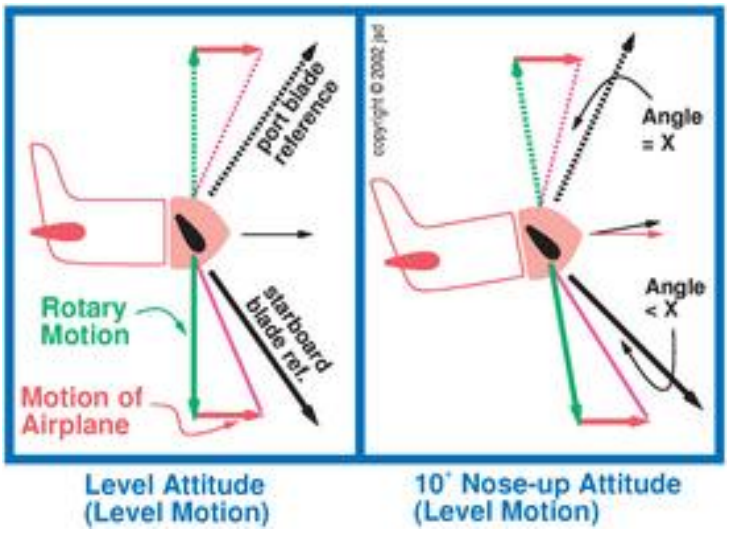

Figure 3. 1 P-Factor example

This has the effect of bending or side loading the crankshaft every 180 degrees with the maximum force when the descending blade is at its greatest angle of attack to the relative wind.

Gyroscopic forces oppose a change in direction. In maneuvering aircraft, the rotating propeller presents a gyroscopic force on the crankshaft that tends to oppose any change in direction of the aircraft. Although there is an additional force caused by the gyroscopic (precession) force, this force is small and is not considered to be a contributing factor in the crankshaft breakage.

Torsional force is the twisting force experienced by the crankshaft. There are two sources of torsional forces: the force that is imposed by the drag of the propeller in reaction to thrust (Newton's opposite and equal reaction) and the force caused by the power stroke of the engine.

The final type of force that acts on the propeller shaft are those imposed by maneuvering the aircraft. These loads can range from one to three g's in normal flight and up to ten g's momentary shock forces.

One or more of any of these forces may break the crankshaft. This had occurred three times in 2006, and the following picture shows that the area of breakage is directly behind the first bearing behind the propeller hub. Figure 3.2 is a picture of a broken crankshaft.

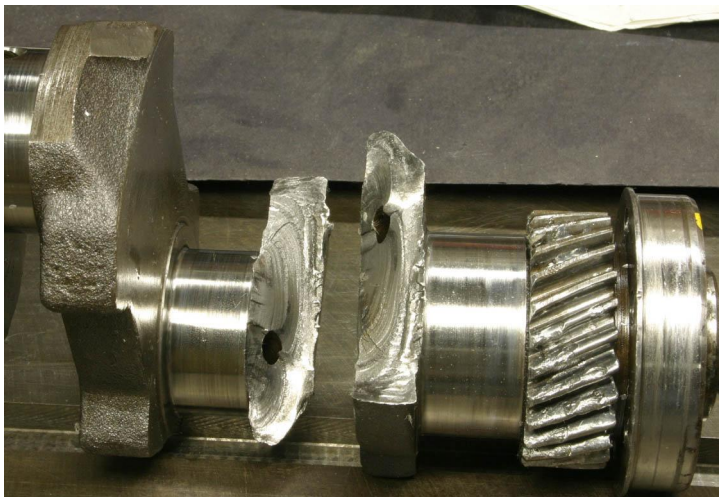

Figure 3. 2 Example of broken crankshaft [16]

Figure 3.3 shows the outline of the Corvair engine modified for aircraft use and the location of the propeller hub and the break. Figure 3.4 shows an actual picture of the engine that experienced two crankshaft failures.

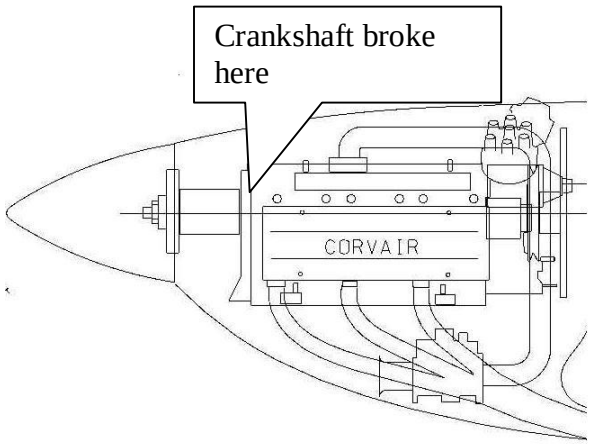

Figure 3. 3 Modified Corvair Outline [17]

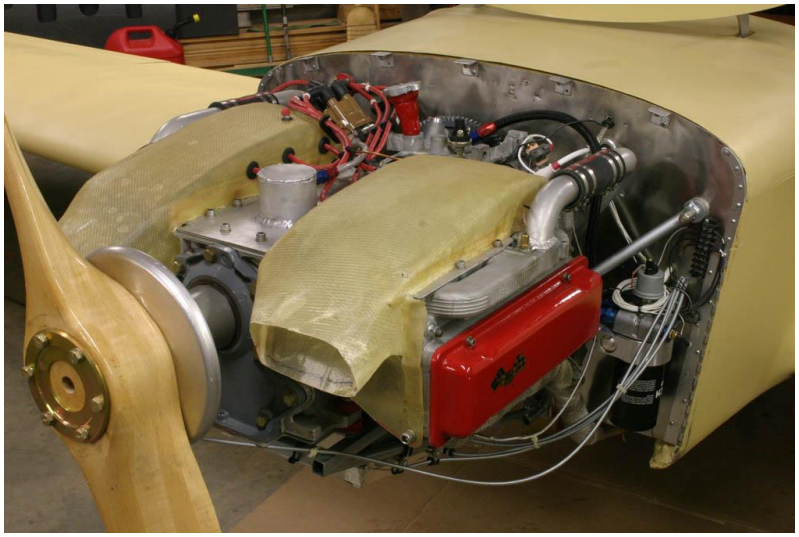

Figure 3. 4 Actual Corvair Aircraft Engine [18]

Understanding the physical location of the failures and having a background in sensors and instrumentation, we can proceed to a discussion of the instrumentation system design.

3.3 Instrumentation Requirements

3.3.1 Environmental Considerations

Environmental considerations for the purpose of instrumentation deals with the environment in which the sensors and recorders must operate to collect data. This section deals with the environment in which the system must survive.

Because there are four distinct sources that could cause the problem with the crankshaft breakage, and because designing one instrumentation system to measure them all would require resources we did not have, we elected to design a system that addressed just one of the possible sources. We chose to measure the bending forces

caused by the rotation of the propeller. Reducing the focus of the instrumentation system to this one parameter narrowed the number of issues to be resolved.

In addition to narrowing the number of parameters that would be recorded, we also needed to design a system that could be installed by non-technical people using regular hand tools. If the system was designed in this manner, it could be shipped around the country, collecting data from many different engines and providing extra depth to the data that we could analyze. Such data would facilitate statistical analysis to either identify the bending moment as the source of the problem or eliminate it.

Several mechanical, aircraft and other engineers have performed basic analysis on these propeller forces. The best described of the group was that provided by Dan Benson of PRS Engineering Services. He performed a theoretical analysis of the loads, an excerpt of which is included here. (The full text is contained in Attachment 2.)

Load Evaluation*:*

M_t = Propeller Shaft Torque, in-lb

W_p = Propeller Weight, lb (10 lb, 62" dia)

W_{fw} = Flywheel Weight, lb (6 lb , 10" dia)

n = Flight Load Factor, g's = 2.5 per FARs

T = Propeller Thrust, lb = max per FARs

ω_y = Yaw Angular Rate = 2.5 rads/sec per FARs

ω_p = Pitch Angular Rate = 1 rads/sec per FARs

Thrust. *The Corvair engine makes 90 hp at 3000 rpm. The relationship between **T**hrust, horse**P**ower, and **V**elocity is:*

T = P/ V

*T = (90 x 33000 /60) / 88 = **562** lb*

....

Load Summary @ 75% Blade Span

Thrust = 281# axial

This axial thrust is the parameter that we want to measure and validate because it is axial thrust that creates the bending moment on the crankshaft. The issue confronting us was how to measure this parameter.

The Corvair engine is a six-cylinder, four-stroke reciprocating engine with a two-blade aircraft propeller mounted directly on the crankshaft. From this information we can determine that we need to look at not only the magnitude of the bending force, but also the frequency of the force since any imbalance in the system will result in a force that will reverse itself at most every 180^{o}.

These force reversals have two principal sources, the propeller and the power stroke of the engine itself. The operating range of the engine is from 600 RPM to 3600 RPM, which translates into a propeller frequency range of 20 Hz to 120 Hz computed as follows:

$$\text{Propeller Frequency} = \frac{600\,\text{Revolutions per Minute}}{60\,\text{seconds per Minute}} =$$
$$= 10\,\text{Revolutions per second} * 2\ \text{force vectors per second}$$
$$= 20\,Hz$$

The power stroke frequency of the engine is computed on the fact that combustion occurs on every second rotation of the crankshaft. For a six-cylinder engine this means that there are three power impulses for every rotation of the crankshaft. This results in a frequency for the engine power pulses of 30 Hz and 180 Hz.

As discussed in Chapter 2, the most common method of determining bending forces in a steel structure is the use of strain gauges. In our case a significant problem exists in how to mount strain gauges on a rotating shaft. In addition to that problem, the area of breakage is directly behind the first bearing following the propeller mount as shown in Figures 18 and 19. Placing strain gauges on the crank cheeks would be very difficult, requiring skills beyond the abilities that could be expected from an average engine builder. Another method is needed to determine what the forces actually were on the engine's crankshaft.

3.3.2 General Requirements

With this information we can generate a basic set of requirements for the instrumentation system. These are the criteria used to design the system described in the following sections. The system

1. must be able to measure forces in excess of 400 inch pounds of force (200 pound engine by up to 2 inches of displacement),
2. must be able to measure frequencies up to 200Hz,
3. must be able to be installed on engines easily by non trained personnel,
4. disassembly of the engine should not be required to install sensors,
5. must be able to be operated successfully by non-skilled personnel,

6. must be able to be shipped at reasonable cost throughout country,
7. must provide tools to analyze recorded data both at test sight and by other analysts, and
8. Must be affordable.

3.4 The Design

With these requirements now identified, we designed the system by first selecting the sensors and identifying the basic interfaces along with the various buy versus build decisions.

3.4.1 Bending Sensor

The first design problem to solve was the problem of measuring the bending moment on the crank. It is obvious from requirements numbers 3, 4 and 5 that the application of strain gauges was not an option. While there are methods of placing sensors inside of an operating engine, this typically is performed in a special facility, and the engine is so heavily modified that it could not be returned to service as an aircraft engine. So the question was how do we solve this problem?

Newton and his three laws of motion offer assistance.[19]

> **I. Every object in a state of uniform motion tends to remain in that state of motion unless an external force is applied to it.**

II. The relationship between an object's mass *m*, its acceleration a, and the applied force *F* is *F* = *ma*. Acceleration and force are vectors (as indicated by their symbols being displayed in slant bold font); in this law the direction of the force vector is the same as the direction of the acceleration vector.

III. For every action there is an equal and opposite reaction. [19]

It is the application of second law that aided us in designing this instrumentation system. Since the mass (*m*) of the reciprocating engine is known during operation and we can measure the acceleration (*a*) using accelerometers, the force (*F*) acting on the engine can be computed using the second law. As described in Section 2.2.1.2 traditional accelerometers are subject to damage under high shock loads. For this application, the thermal accelerometer described in Section 2.2.1.2 provides the high sensitivity while remaining immune to large shock loads. This provides the most robust method of measuring the accelerations. This device does present a problem in that its native frequency response is from 0 to 30Hz which is substantially below the 180 Hz specified in Section 3.3.1. This required special signal conditioning to extend the range to at least 200 Hz to cover the entire range of interest. This subject is described in greater detail in Chapter 5.

The next required sensor determines engine RPM. We would like to compare the force frequencies over engine RPM. Knowing the engine RPM allows us to look for harmonics in the system. We selected the snap on inductive pickup from an automotive timing light to keep installation as simple as possible. This could be clamped around a coil lead, and the RPM could be determined by dividing the spark frequency by 3.

3.4.2 Signal Conditioning

Having now selected the sensors, we now turn to signal conditioning. To make the job as easy as possible and to reduce the amount of custom circuit boards that would have to be designed, we located a surplus sixteen channel signal conditioning board with a 12 bit analog-to-digital converter built by IO Tech. This board, a DaqBoard100^{TM}, provided nearly all of the signal conditioning required for the project. An advantage of this device was that it connected to the parallel port of a computer and could transfer data fast enough to supply 512 samples per channel per second. This easily exceeded the Nyquist Sampling Theorem [20] requirement that the data be sampled at twice the maximum frequency of interest. In our design we needed to be able to take samples at minimum rate of 2 * 180 Hz or 360 samples per second. The signal conditioning board came with software drivers that could be integrated with data logging software that allowed the data to be recorded directly to disk in real time.

There were two design issues that remained to be resolved for signal conditioning. This first was that the accelerometers had a 3db frequency of 30 Hz, which was well below our need for 180Hz. The frequency range of this device needed to be extended to meet the requirements of the project, so a custom board needed to be designed to perform this function. The second task was to design a circuit that would take the spark signal from the inductive pickup and convert it to a signal level that could be recorded by system.

The design for these signal conditioners is shown in Chapter 4, which describes, and documents the entire hardware system, interconnection diagram and printed circuit board layouts.

3.4.3 Data Recorder

The DaqBoard simplified the selection of a data recorder. Since the drivers for the acquisition board were software compatible with languages that ran on Windows 98, a laptop was procured on Ebay for less than $150 that came with the operating system and a hard drive of sufficient capacity to perform the role of recorder. The software that was developed for the data recorder is described in Chapter 5.

Chapter 4 Hardware Design

Most of the signal conditioning is contained in the DAQ Board. However, the output from the accelerometers must be amplified and the frequency range needed to be extended. In addition to the signal conditioning required for the accelerometers, signal conditioning is required for the inductive pickup used for RPM measurement. Figure 4.1 is the block diagram of the instrumentation system designed for this application.

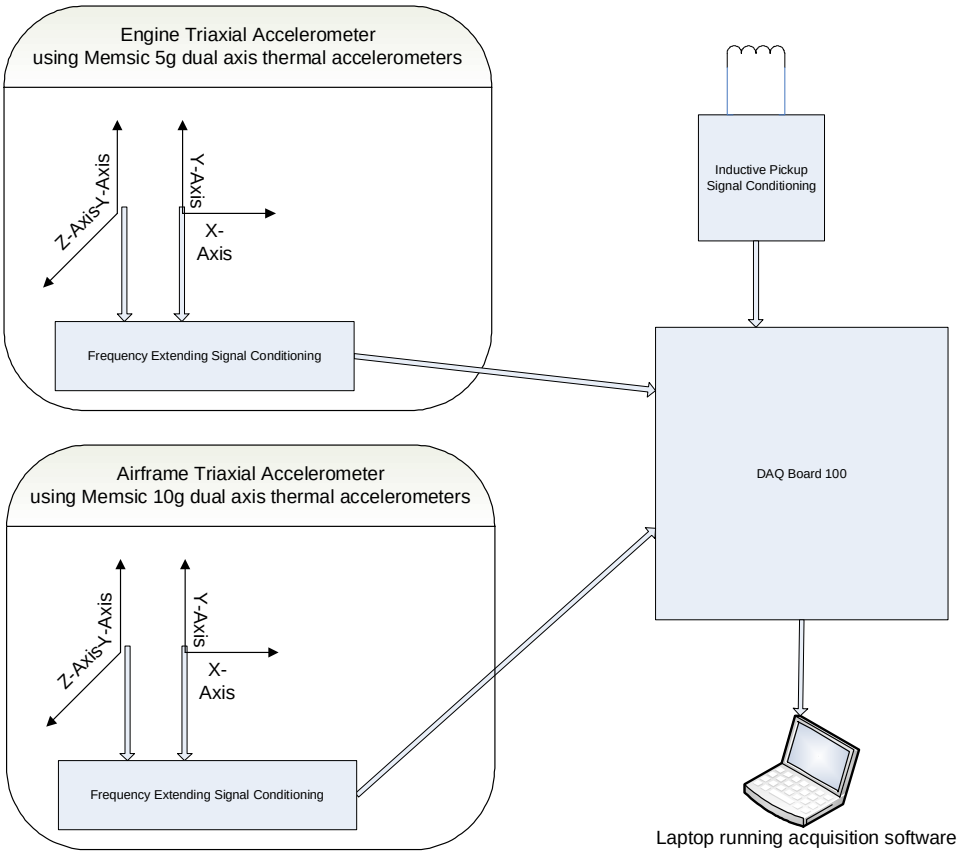

Figure 4. 1 Instrumentation and Measurement System [21]

The dual axes thermal accelerometers are mounted on a PC card along with its signal conditioning and two cards are mounted in an enclosure to create a triaxial

accelerometer with the vertical or “y” axis duplicated. Two of these sensor chassis were developed to provide the capability to measure data from both the engine and the airframe. This will allow for transfer functions to be performed in the future, potentially collecting data in flight.

4.1 Accelerometer Signal Conditioning

After reviewing several “off the shelf” accelerometers, we did not find any that would meet the environmental requirements and measurement dynamics required for mounting on a running aircraft engine. This was due to momentary shock loads of 100g that may last 0.1 to 0.2 seconds and a maximum dynamic range of +/- 6g and an expected maximum magnitude of +/- 1.5g from 20 Hz to 180 Hz. Chapter 3 described the reasons for selecting thermal accelerometers. These accelerometers directly support measurements from 0 to 30Hz without any signal conditioning. This frequency response is far less than that needed for our application, requiring additional signal conditioning that will provide a flat frequency response up to 200 Hz with at lest 3 dB of attenuation at 250 Hz.

Memsic Corporation, the manufacturer of the thermal accelerometer, provided a reference design for this device to extend the range well beyond 160 Hz. This application note and reference design is contained in Attachment #3. Using that reference design and careful layout, we have extended the range to 200 Hz and validated the performance using a calibrated test stand. Figure 4.2 is the schematic of the Sensor Board with Figure 4.3 showing the Copper layout of the board, Figure 4.4 showing the Silk screen, Figure 4.5 is a picture of the actual boards and Figure 4.6 is a photo of the assembled sensor.

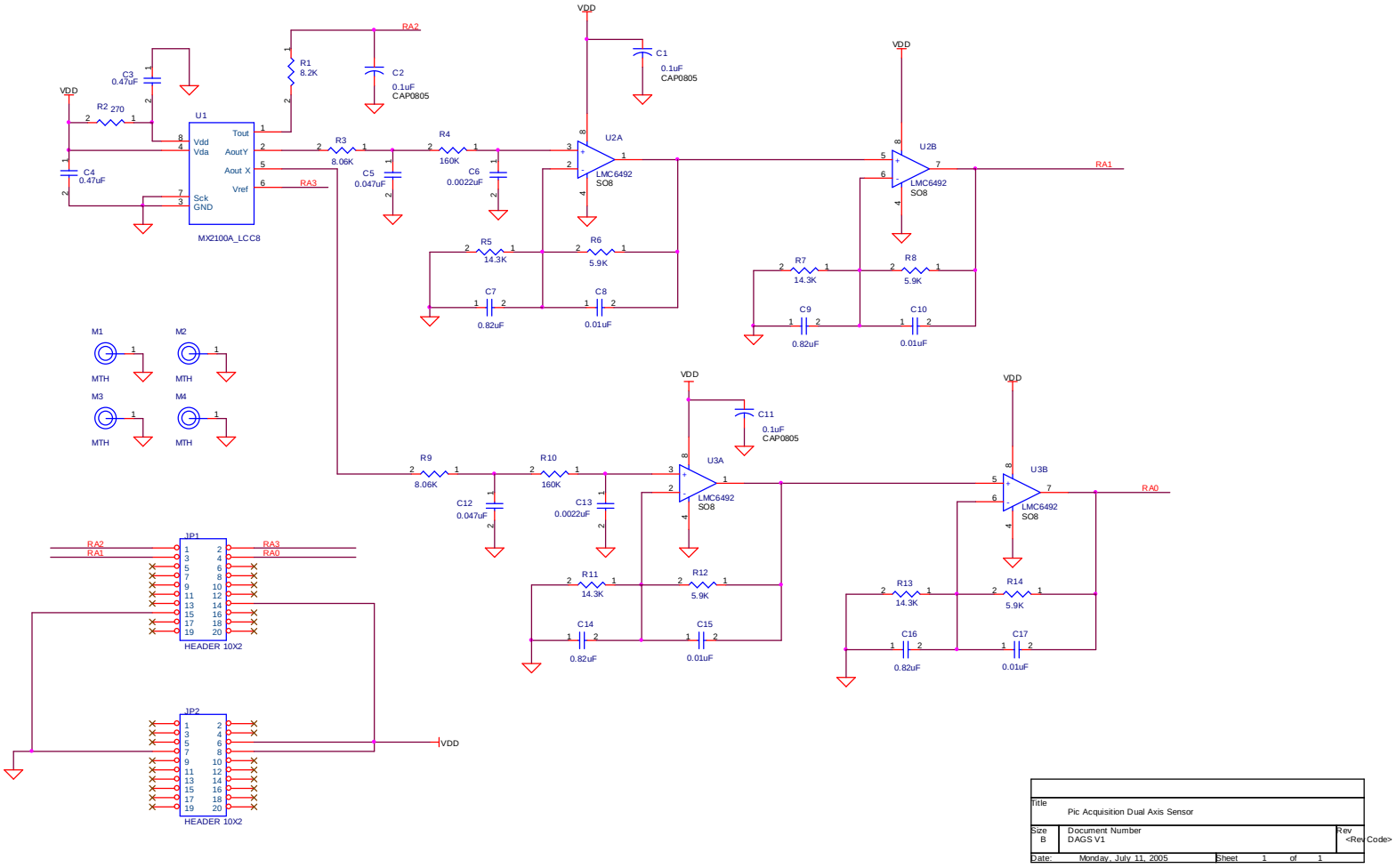

Figure 4. 2 Schematic of Dual Axes Sensor Board [22]

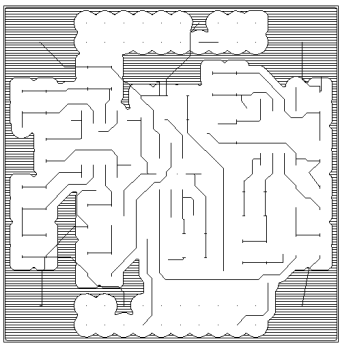

Figure 4. 3 Circuit Board Copper Layout [23]

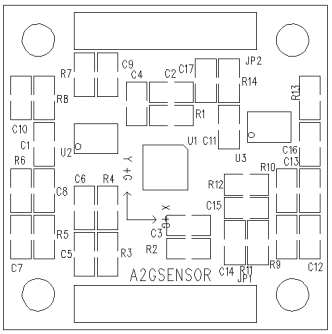

Figure 4. 4 Circuit Board Slik Screen [23]

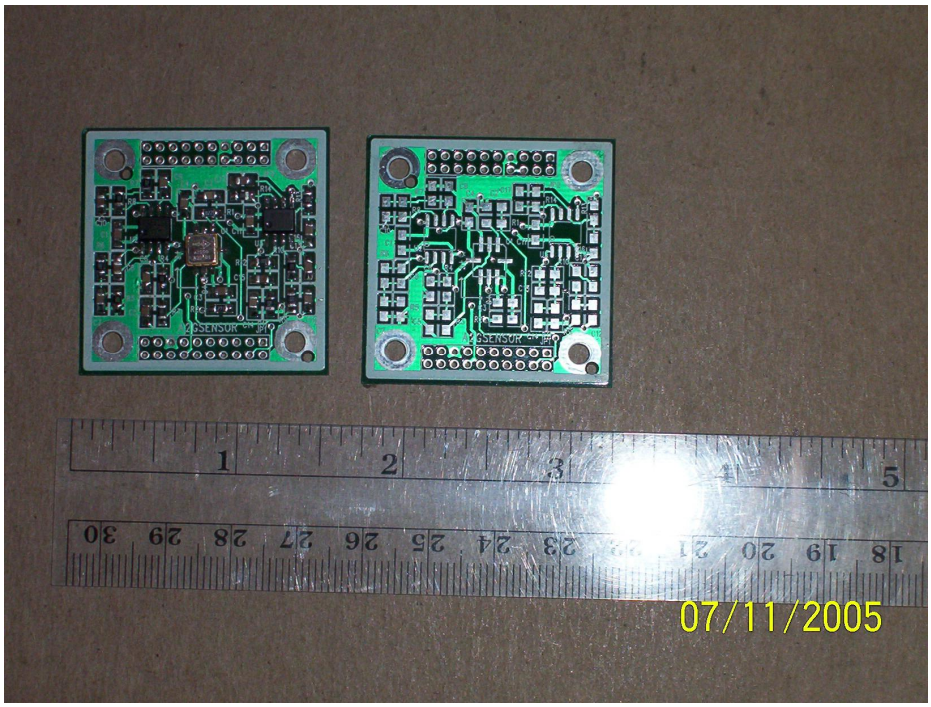

Figure 4. 5 Photo of Actual Dual Axes Sensor Board

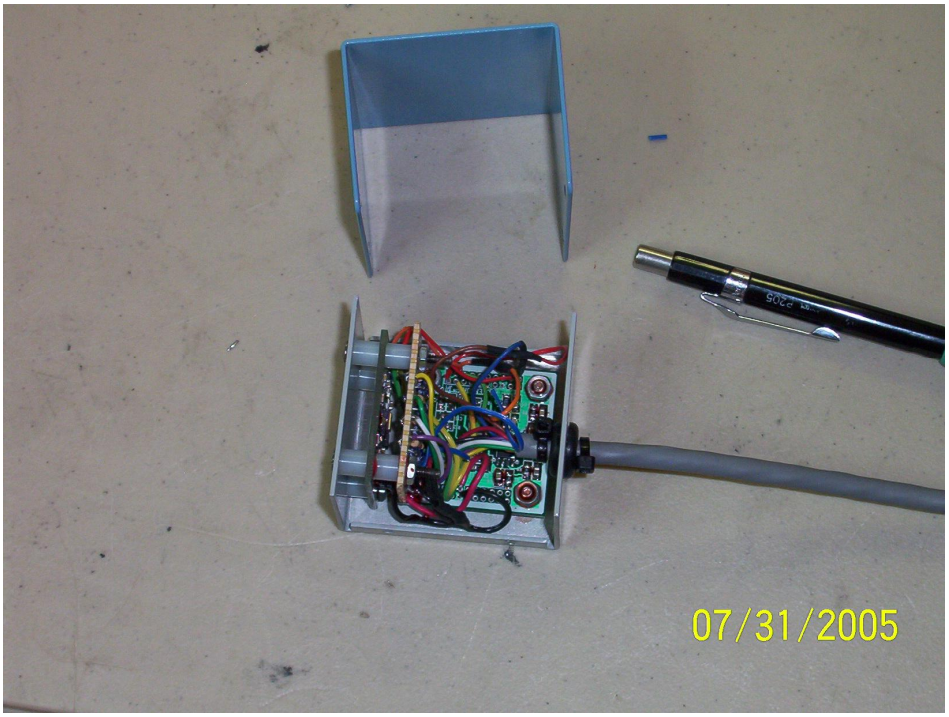

Figure 4. 6 Photo of assembled Triaxial Sensor with two Dual Axes sensor Boards

Two of these sensor assemblies are connected to DAQ Board 100. The output of the calibration of these sensors is contained in ATTACHMENT 1.

4.2 RPM Inductive Pickup

The RPM Inductive pickup was an actual inductive pick up for a timing light. It was wired into a simple comparator circuit to provide a square wave signal that would represent the running frequency of the engine by recording the firing pulses to the distributor. Figure 4.7 is the schematic of the inductive pickup circuit.

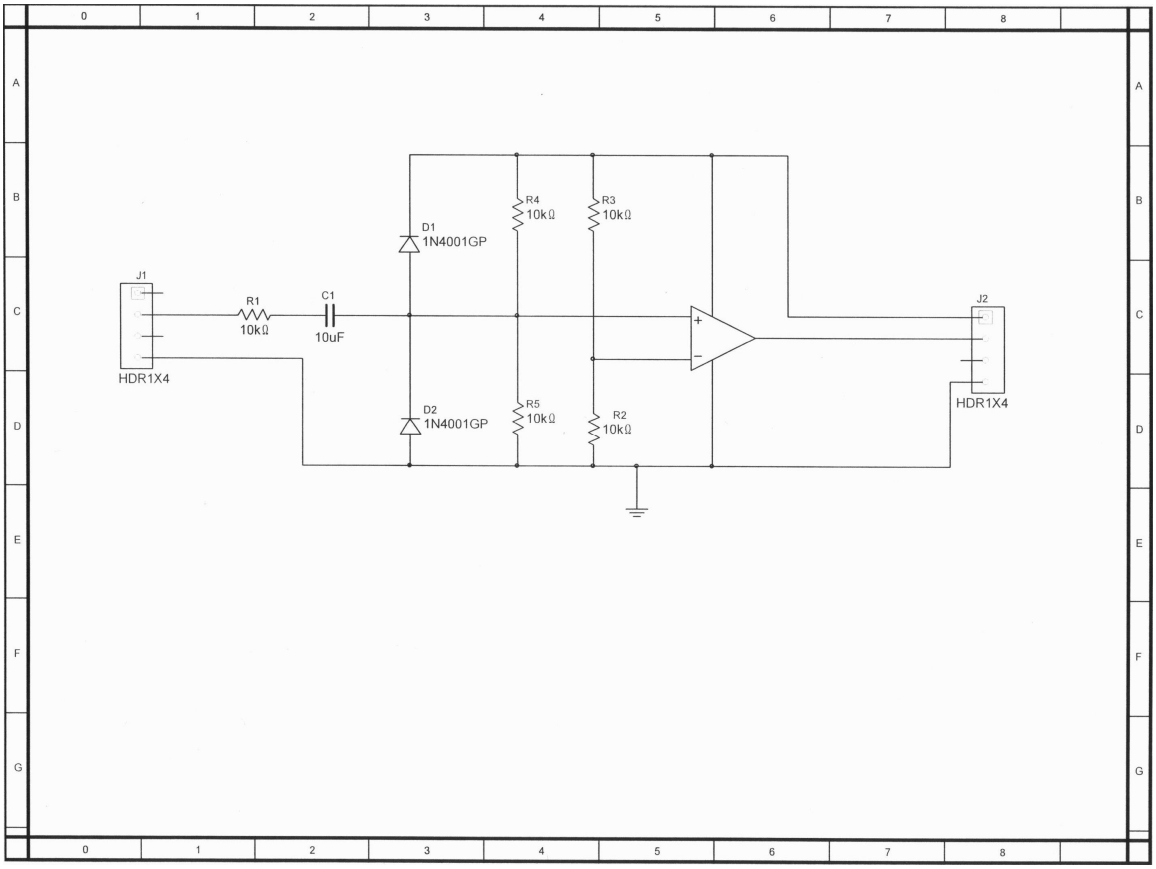

Figure 4. 7 Inductive Pick Up Signal Conditioning circuit diagram [6]

This circuit is a simple comparator that fires an output when the trigger from the input changes the + terminal of the operational amplifier. The negative terminal is held at the reference value as determined by R3 and R2. The input is coupled through C1 and the input is clamped by the diodes D1 and D2 to clip the signal should it exceed the input voltage (5volts) or ground. It is possible to have a signal whose potential is less than ground due to the nature of reactive devices. The output of this circuit is connected to the DAQ Board 100 as described in the following Section.

4.3 Final Signal Conditioning and Digitizing

The DAQ Board 100 has general amplifiers that provides gains of 1,2,5,10,and 20 under software control. The output of these gain stages are connected to a 16 channel MUX that acts as a switch to the 12 bit Flash Analog to Digital Converter. Eight of the sixteen channels are assigned to the two triaxial accelerometer g outputs, six to monitoring signals and one assigned to a tachometer input. The signal configuration or channel assignment for the A/D converter is as follows:

1. Engine Longitudinal
2. Engine Lateral 1
3. Engine Vertical
4. Engine Lateral 2
5. Engine Accelerometer Temp1
6. Engine Accelerometer Temp2
7. Sensor Voltage Reference
8. RPM
9. Airframe Longitudinal
10. Airframe Lateral 1
11. Airframe Vertical
12. Airframe Lateral 2
13. Airframe Accelerometer Temp 1
14. Airframe Accelerometer Temp 2
15. Airframe Sensor Voltage Reference
16. Unused

This unit is connected to a laptop computer to record the digital data and to allow quick review of the acquisition data. Figure 4.8 is a picture showing the analog to digital converter which is connected to a laptop to collect data for post processing.

Figure 4. 8 Photo of DAQ Book ™ 100

This hardware records data at the rate necessary to determine the forces acting on the engine. A program was developed that controls the recording of the data. The rate at which the recorder gathers data is defined as the sample rate. As described in Chapter 3 a six-cylinder engine has three power strokes per revolution. The operational RPM range of the engine is 600 to 3600, which results in a power stroke frequency of 30 Hz to 180 Hz. With a two-blade propeller the displacement forces over the same RPM range results in a frequency of 20 Hz to 120 Hz. Based on the Nyquist rate [20] for discrete sampling theorem we need to sample at least 2 times the frequency of interest. For this application, the sample frequency selected was 512 Hz, which is more that 2.5 times the maximum frequency of interest.

The software programs that gathered the data and performed post analysis are described in the next Chapter.

Chapter 5 Software Design

There are five sequential software operations required to extract the magnitude forces from the system. These steps are:

1. to record time history data,
2. to filter the recorded data,
3. to convert data from time domain to frequency domain,
4. to correlate data from all three axes and
5. to convert results into force magnitudes

Each of these operations has unique requirements and introduces its own errors. This paper will describe each of the operations, identifying the design of the software and the results obtained.

5.1 Record Time History Data

The hardware described in Chapter 4 is able to record data at the rate necessary for the task of determining the forces acting on the engine as described in the previous chapter. A program was developed that controls the recording of the data. The program records the data across all sixteen channels and stores the information in binary form in a removable flash drive. This allows the data to be mailed back to the author for analysis while the system is shipped to other builders desiring to measure their engine installations.

5.2 Filtering Recorded Data

Since the rate of change occurs at a much slower rate than the sample rate it is necessary to provide initial filtering to remove any high frequency information and retain the trend information that falls within the frequency of interest. The acquisition program on the recorder computer provides a software filter using a boxcar format that is in addition to the hardware filters. A noncausal averaging system is used and is more commonly referred to as a SINC filter and is represented as follows:

$$y[n] = \frac{1}{2M+1}\sum_{k=-M}^{M} x[n-k]$$

or the more common form for 3 *elements* [24]

$$y[n] = \frac{x[n]+x[n-1]+x[n-2]}{3}$$

A combination of hardware and software filters provides the best filtering techniques while minimizing the ultimate phase shift. This system was used to record data from several engines to create a data base of time history data and allows the development of the post processing programs. Figures 5.1 and 5.2 are sample plots of 1 second of time history data from a representative engine.

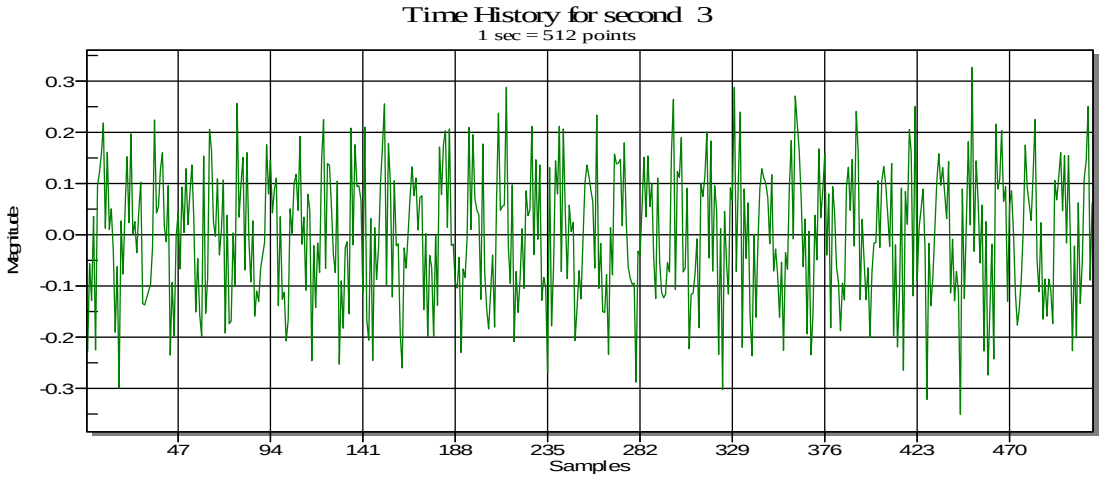

Figure 5. 1 Time History Data Plot for second 3 [25]

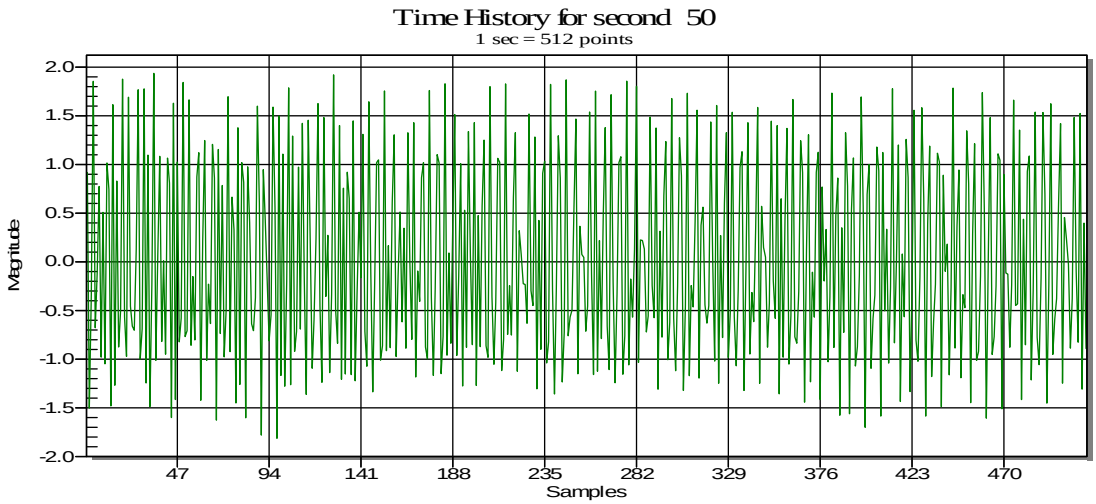

Figure 5. 2 Time History Data Plot for second 50 [25]

These data samples were taken from an engine that was accelerated from idle which is approximately 600 RPM to maximum RPM which is around 3,000 RPM. This data was collected utilizing the filters described above and the individual data points were moved into a data base. The data base records consist of the following data items and resolution:

- Sample Count uint32
- Engine Vertical Acceleration double
- Engine Longitudinal Acceleration double
- Engine Lateral 1 Acceleration double
- Engine Lateral 2 Acceleration double
- Airframe Vertical Acceleration double
- Airframe Longitudinal Acceleration double
- Airframe Lateral 1 Acceleration double
- Airframe Lateral 2 Acceleration double
- RPM single

The data base selected is Microsoft's SQL Server to allow the development of stored procedures and to allow the use of Microsoft Visual Basic to provide a rapid method of developing user interfaces. Visual basic is designed to directly interface with the SQL Server and contain native data base utilities that simplify the ability to scan, iterate and extract data from very large tables. An average data collection run lasts from two to four minutes at 512 samples per second which results in an average data set of 61,000 to 122,000 records, so the ability to rapidly and natively access the records is important to the ability to process the data into its final form for analysis.

5.3 Convert Time Domain Data to Frequency Domain

The primary method of converting time history discrete data into the frequency domain is to use Fourier transforms. The method selected for this application is based on the description and examples contained in "Fourier Series Representation of Discrete-Time Periodic Signals". This utilizes the basic concept of linear combinations of harmonically related complex exponentials. By definition, for a signal to be periodic, the signal must have a component that repeats itself. This is represented by the form:

$$x[n] = x[n+N] \text{ [26]}$$

For this equation to be true, the smallest interval (highest frequency) is the smallest possible number of N. Therefore the fundamental frequency can be expressed as:

$$\omega_o = \frac{2\pi}{N} \text{ [26]}$$

Given the complex exponential $e^{j\left(\frac{2\pi}{N}\right)n}$ which is periodic with period N, the set of all discrete-time complex exponentials are:

$$\phi_k[n] = e^{jk\omega_o n} = e^{jk\left(\frac{2\pi}{N}\right)n} \text{ for k = 0, +/- 1, +/-2,….[26]}$$

Since ϕ_k is distinct and unique only over a range of N, it is not necessary to have k values extend beyond +/- N. Taking the general representation of the periodic signal in terms of linear combinations of the discrete-time complex exponentials we can develop the discrete time Fourier series for the signal.

$$x[n] = \sum_{k=\langle N \rangle} a_k \phi_k[n] = \sum_{k=\langle N \rangle} a_k e^{jk\omega_o n} = \sum_{k=\langle N \rangle} a_k e^{jk\left(\frac{2\pi}{N}\right)n} \quad [27]$$

The a_k terms are the Fourier coefficients of the signal. The magnitude of these coefficients can be determined from the source signal by using the inverse form as follows:

$$a_k = \frac{1}{N} \sum_{n=\langle N \rangle} x[n] e^{-jk\omega_o n} = \frac{1}{N} \sum_{n=\langle N \rangle} x[n] e^{-jk\left(\frac{2\pi}{N}\right)n} \quad [28]$$

Converting this formula to program code and processing the time history data for one second (512 samples), the resultant data set is two data arrays of 256 elements. They are the real part and the imaginary parts of the complex result of the operation. Each element of the array represents a discrete frequency based on the sample rate. Since our sample rate is 512 samples per second and the Nyquist rule applies, the resultant element value is 1 Hz and a total dynamic range of 256 Hz. The following figures show the real and imaginary components of the two signals shown in Figures 5.3 and 5.4.

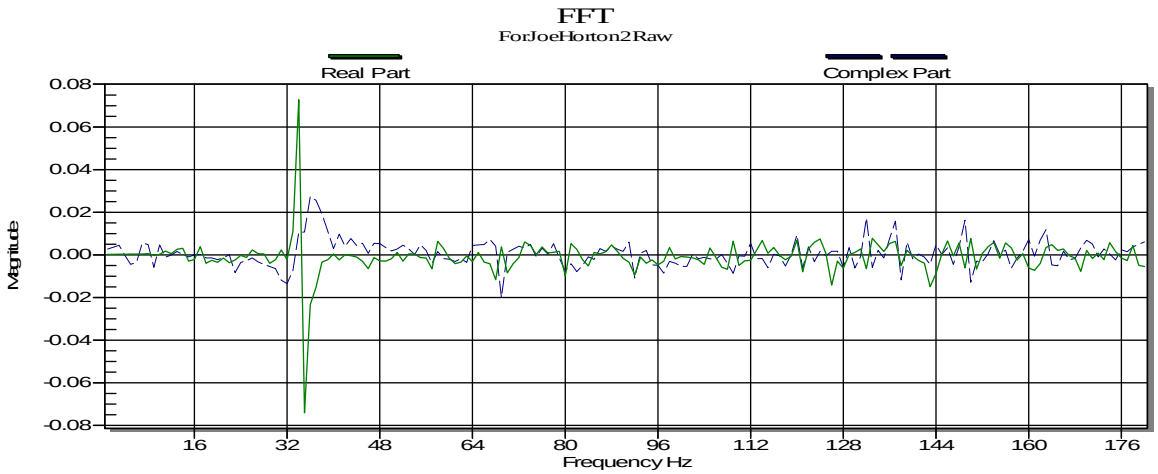

Figure 5. 3 Real and Imaginary Plot for second 3 [25]

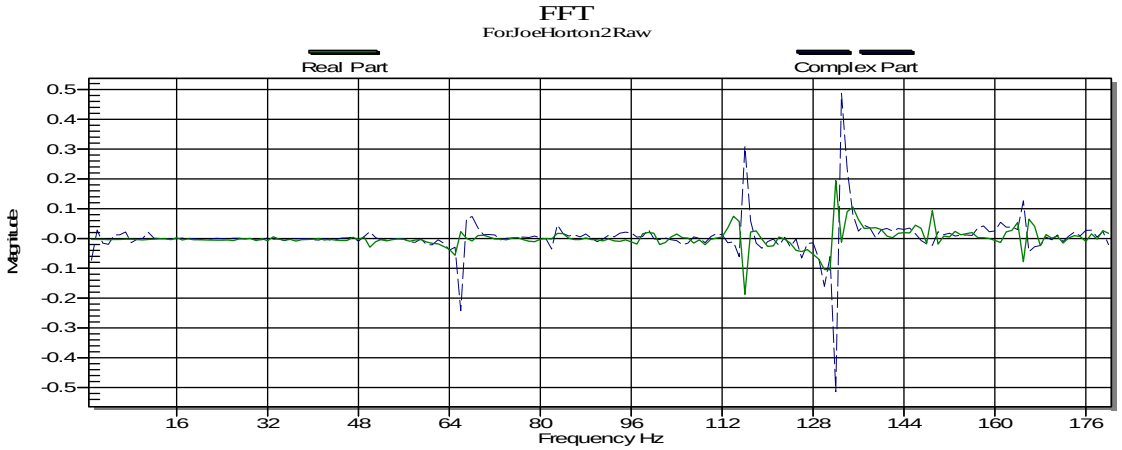

Figure 5. 4 Real and Imaginary Plot for second 50 [25]

Taking these plots and combining them according to the Fourier process for magnitude as follows:

$$y[n] = \sqrt{\mathrm{Re}[n]^2} + \sqrt{\mathrm{Im}[n]^2} \quad [29]$$

Based on this formula the resultant magnitude plots for the signals shown in Figures 5.1 and 5.2 are in Figures 5.5 and 5.6 respectively:

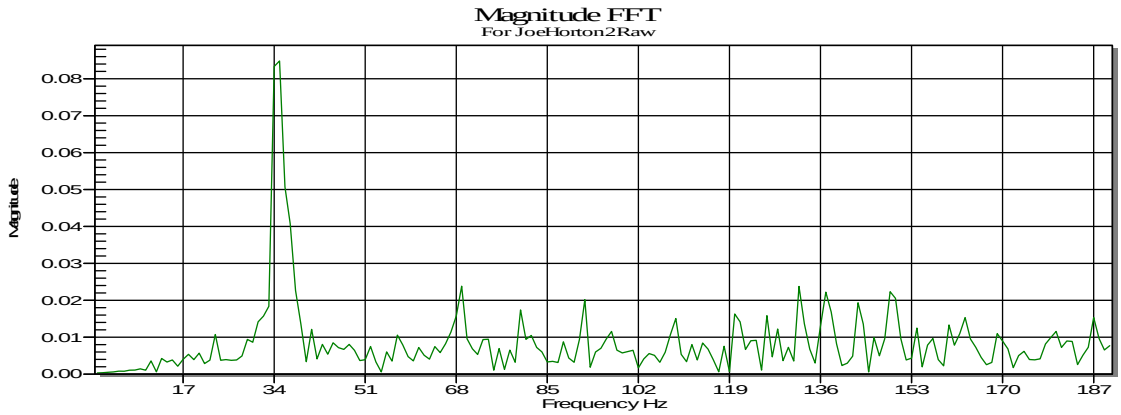

Figure 5. 5 Magnitude Plot Second 3 [25]

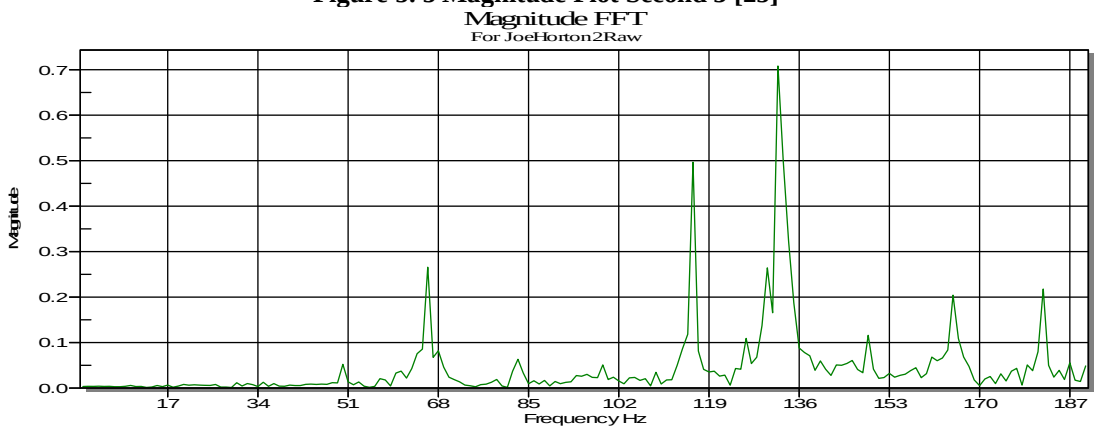

Figure 5. 6 Magnitude Plot for second 50 [25]

5.4 Correlating Data from All Three Axes

The figures showing the Fourier transforms above were selected for their clarity to highlight the basic principals utilized in this analysis. It should be noted that the majority of the transforms do not allow for such clear identification of peak values. Figure 5.7 is a more typical plot of the transform output.

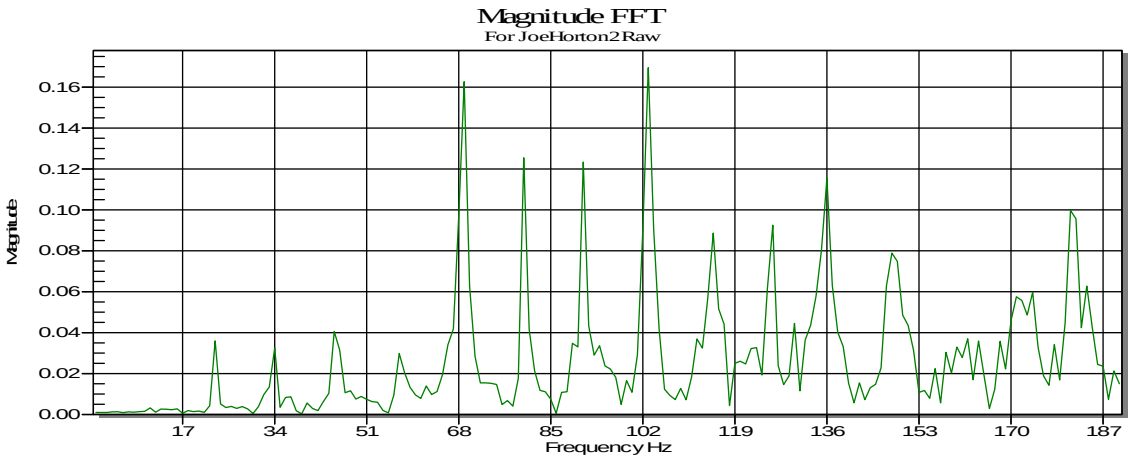

Figure 5. 7 FFT output with noise from Vertical Accelerometer [25]

This plot shows the difficulty in determining which peaks are the result of input forces and which peaks are sensor noises or harmonics. To eliminate those peaks that are not the principle frequencies (propeller and power strokes), it is necessary to perform a correlation of the three axes measurements. For example let us compare the longitudinal (Figure 5.8) and lateral (Figure 5.9) axes FFT plots for the above vertical plot.

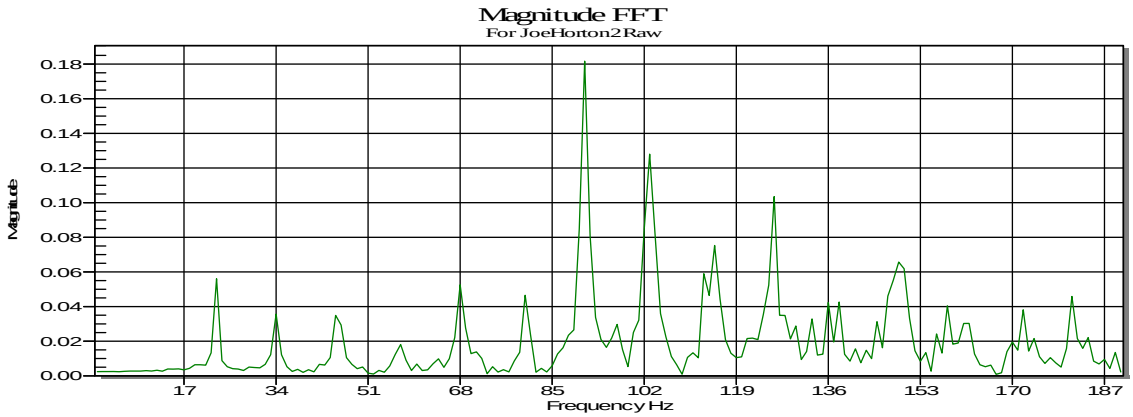

Figure 5. 8 Longitudinal Accelerometer FFT Plot for the same second as Figure 5.7 [25]

It can be observed that peaks near 68Hz and 102Hz appear to correlate exactly between the vertical and longitudinal axes. Now looking at the lateral axis we get the following plot.

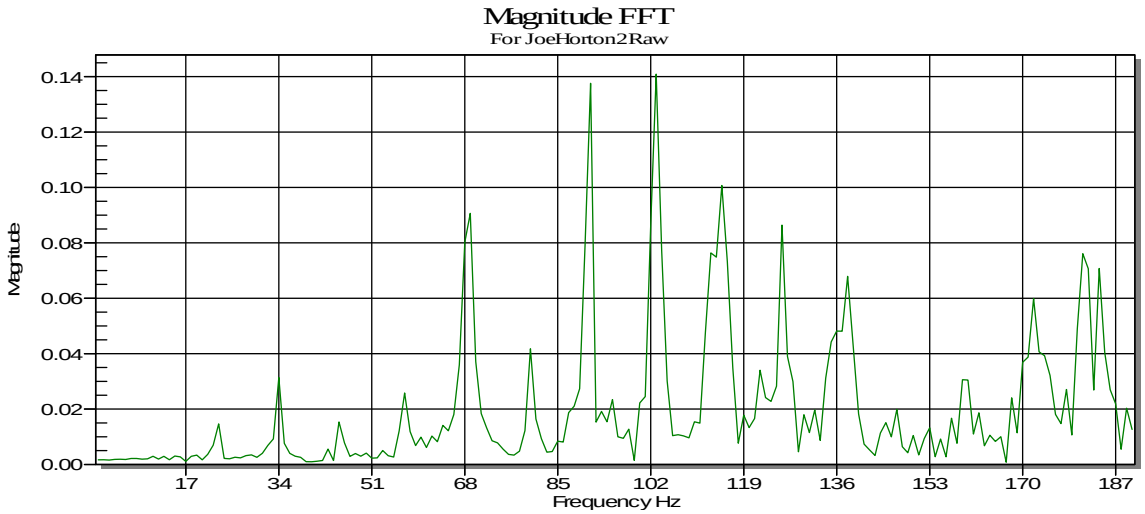

Figure 5. 9 Lateral Accelerometer FFT Plot for the same second as Figure 5.7 [25]

Here the correlated peaks are near 68 Hz and 102 Hz. These frequencies correlate to our 2:3 ratios for engine and propeller forces as follows.

68 Hz / 2 pulses per rev (propeller) = 34 Revolutions per second

102 Hz / 3 pulses per second (engine) = 34 Revolutions per second

By correlating the peak values it is possible to determine the RPM as well as identifying damaging harmonics. Random impulses are not of concern in our analysis, however harmonic inputs are. It is the harmonic impulses that create bending moments in the shaft and are carried at the input to the first bearing as well as between the first and second bearings.

The differences in the acceleration magnitudes are due to the mounting of the engine on the airframe. When performing the correlation it is necessary to normalize magnitude

of the data. This is accomplished by selecting the absolute peak for each axis, determining the axis that has the largest peak, and then multiplying the other two axes by a factor that will result in each axis's peak value to be equal to the others.

Fm[n] = Fm[peak] / Maximum Peak Value

Used to normalize low peak channels

The next step is to add the axes frequency bins together to develop a correlated peak value for that period and then select the top two values. These top two values should be the propeller and the engine power pulses. This process resulted in the plot shown in Figure 5.10.

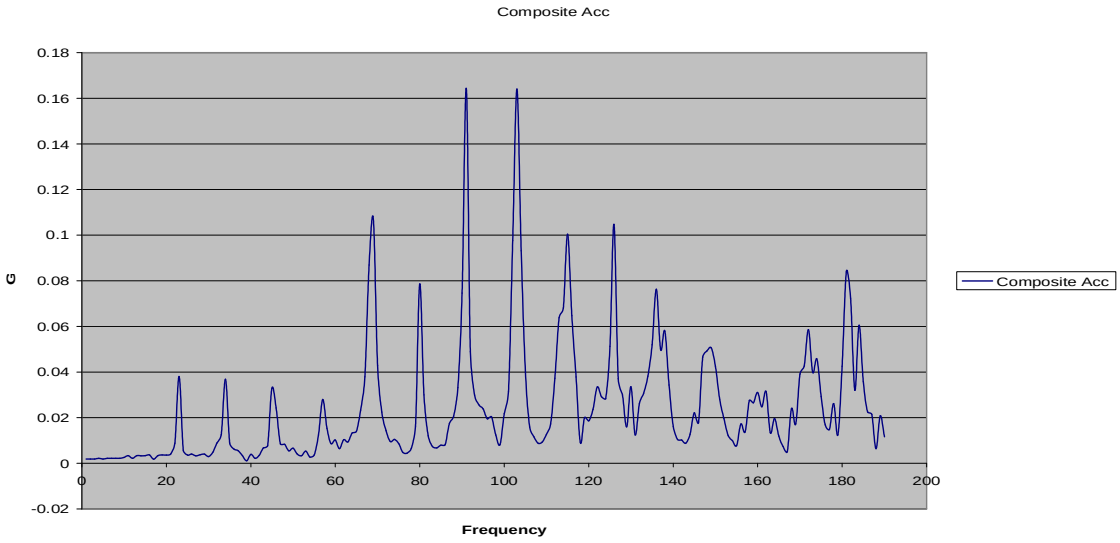

Figure 5. 10 Composite Magnitude Acceleration FFT [30]

There are three dominate peaks shown in this plot at 69 Hz, 91 Hz and 103Hz. The peaks at 69 Hz and 103 Hz should be the propeller and engine power stroke inputs to the system. An interesting peak is occurring at 91 Hz that does not seem to correlate to

any expected mechanical frequency. If this peak is duplicated in further processing, it will indicate an unexpected input that will require further study.

5.5 Convert Results into Force Magnitudes

The final stage is to create a “Time History of Magnitudes” (Figure 5.11). This plot shows an overview of the magnitude of forces over the duration of the test. This gives a three dimensional approximation of the forces since the mass of the engine system remains constant in our formula for force. ***F=ma***.

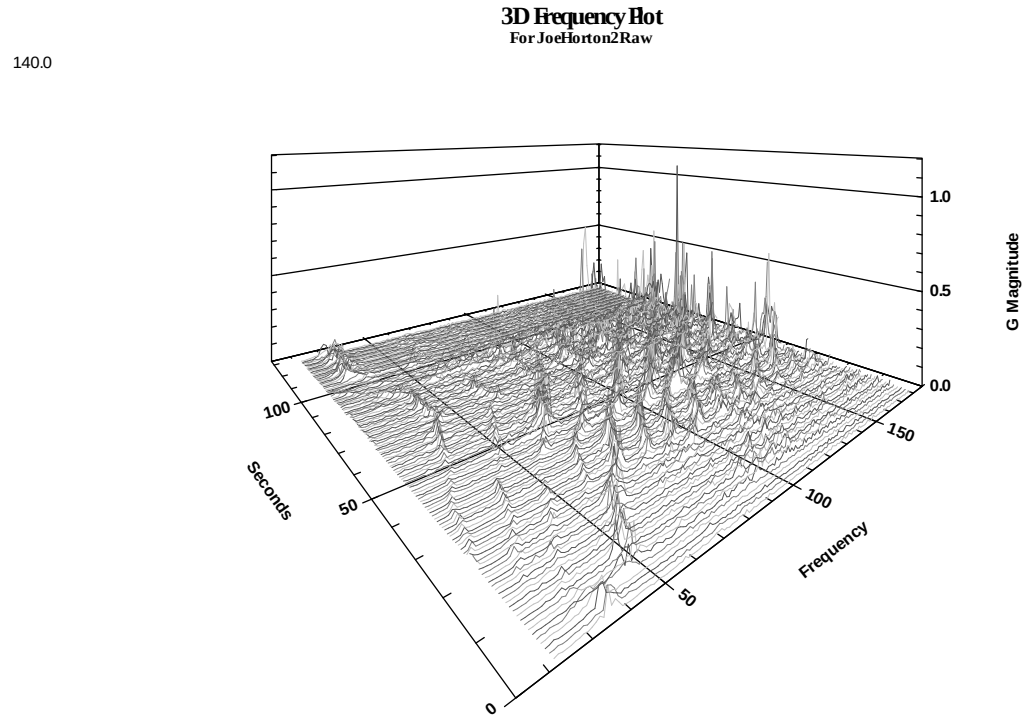

Figure 5. 11 "Time History of Acceleration Magnitudes" [25]

The software developed for this application allows this plot to be rotated 360^{o} along the x axis and $^{+}/_{-}$ 90^{o} along the y axis. This allows closer examination of either a specific

time or a specific frequency. As the engine RPM increase, several harmonic vibrations occur about 20 seconds into the test. This can be seen by the quantity of peaks appearing on the graph as one moves along the Seconds axis in an increasing direction.

While the peak magnitudes of the “g” forces appear to increase with frequency as shown on the chart, the overall effective power of the forces at those frequencies is reduced due to the minimal time that the system is exposed to the peak value. For example Table 5.1 shows the relative displacement of the engine based on a 1g input as frequencies increase.

Table 5.1 Displacement at 1g

Frequency	Acceleration	Displacement	Mass	Force	Work
Hz	**mm/s^2**	**mm**	**kg**	**Newtons**	**Jules**
20	19613.4	1.2420	99.79	1957	2.4309
30	19613.4	0.5520	99.79	1957	1.0804
50	19613.4	0.1987	99.79	1957	0.3889
75	19613.4	0.0883	99.79	1957	0.1728
100	19613.4	0.0497	99.79	1957	0.0973
125	19613.4	0.0318	99.79	1957	0.0622
150	19613.4	0.0221	99.79	1957	0.0433
175	19613.4	0.0162	99.79	1957	0.0317
200	19613.4	0.0124	99.79	1957	0.0243
Hz	**inches/s^2**	**inches**	**lbs**	**Pound-Force**	**Inch Pound-force**
20	386.09	0.024449	220	439.9	10.7551
30	386.09	0.010866	220	439.9	4.7800
50	386.09	0.003912	220	439.9	1.7209
75	386.09	0.001739	220	439.9	0.7650
100	386.09	0.000978	220	439.9	0.4302
125	386.09	0.000626	220	439.9	0.2754
150	386.09	0.000435	220	439.9	0.1914
175	386.09	0.000319	220	439.9	0.1403
200	386.09	0.000244	220	439.9	0.1073

(Note: English units are for reference only and were derived from the si units)

From this table it is obvious that the higher the frequency, the less the delta distance is required to meet the 1g of acceleration. This means that the relative energy required

to move the engine that amount is considerably less. This is based on the formula ***W = Fd***.

Further analysis need to be performed to determine if the variance in frequency is due to the durometer of the rubber mount. A further calibration may be necessary to determine the actual force required to move the engine in the mount and apply that factor to this analysis.

5.6 Error Analysis

A comprehensive error analysis has not been performed but the following error sources have been identified and an attempt at quantification of the potential error has been performed. The following paragraphs describe the error sources and their contribution to the overall error figure for the system.

5.6.1 Sensor Errors

The sensors used for this project are Memsic Corporation thermal accelerometers with a $^{+}/_{-}$ 5g range absolute. Absolute accelerometers actually measure the force of gravity and can be calibrated by noting the output values perpendicular to the ground then rotating the unit 180^{o} and noting the new value. The difference between the two measurements is divided by 2 g to get a $^{volts}/_{g}$ value. If a precision angle measurement tool is used to measure different angles of the accelerometer in relation to the force of gravity, the linearity of the accelerometer can be determined. For example if the accelerometer is placed perpendicular to the gravity force line the accelerometer should indicate 0 g. The error sources for this device are as follows: [31]

- Nonlinearity 1% Full Scale
- Alignment error $^{+}/_{-}$ 1^{o}
- Transverse Sensitivity $^{+}/_{-}$ 2% Full Scale
- Noise 1.0 mg/Hz

The largest error here is the transverse sensitivity at 2%. This means that an acceleration that appears on the transverse axis to the primary axis may have up to a 2% coupling error. This relates to a 4% error of the current magnitude. Example:

Current reading	300mv
Uncertainty $^{+}/_{-}$ 2%	294mv to 306mv
Sensitivity	150 mv / g
Total possible Error	12mv / 150 mv / g = 0.08g or 8mg

5.6.2 Digitizing Error

The next layer of error that can occur are those errors inherent digitizing the analog output from the sensor. This error is $^{+}/_{-}$ ½ the least significant bit of the A/D converter. The range of the A/D converter is 12 bits which resolves to 4096, providing a resolution of 4094 counts. The input range is 0 to 5 volts, so the binary resolution is 0.00122 volts per bit. The dynamic range of the sensor is 0 to 3 volts so the overall resolution of the digitizing system is as follows:

$$\frac{150\frac{mv}{g}}{1.22\frac{mv}{bit}} = \frac{288 bits}{g} or \frac{3.472 mg}{bit}$$

Since the error is $^{+}/_{-}$ ½ LSB the total error here is approximately 3.5 mg.

This value is loaded into a floating point variable for storage so no additional computational errors are anticipated. The data is stored into sequential data base

records for further processing. The errors to this point are additive and are magnitude errors and the total possible error is 3.5 mg + 8 mg ~ 11.5 mg. [32]

5.6.3 FFT Conversion Errors

The final error of the system is that determined by the resolution of each frequency bin of the FFT process. The input to the FFT is 512 samples per second and the output is 256 real and 256 imaginary elements. When these elements are combined, the result is 256 magnitude bins representing 1 Hz per bin. This is based on the fact that the input of 512 samples represents 1 second of data. The result of this process identifies that maximum granularity of the frequency output is 1 Hz and can only be considered the power within a 1 Hz band width. For example if a sinusoidal frequency of 50.25Hz is processed, the entire magnitude will be cumulated in the 50Hz bin. If the frequency is 50.55, the magnitude will be reflected in the 51Hz bin.[33]

Chapter 6 Conclusion

During the course of this project we analyzed the problem and narrowed the focus to allow a cost effective measurement system to be developed. The system was built and the software for both the data acquisition and the post processing was developed by the author.

Generally, the system performed as expected collecting data from five different engines. The software performed without any problems and the acquired data were representative of the input observed on the two test engines that were measured prior to the system being sent to other builders to collect data.

Two major issues were discovered with the system that needs to be addressed. The first issue is that the forces measured and shown in this thesis do not approach the theoretical loads expected. Using Mr. Benson's analysis contained in Attachment 2, we should have expected to see forces in the range of 281 lbs or greater. This did not happen in any of the data collected so far. Additionally, there is evidence of harmonic vibrations at certain RPM ranges; however, none of these approaches a level of force that could be considered damaging to the engine or crankshaft.

This author, based on his personal experience with his own engine, made the assumption that the engine could be considered as a "free body" exposed to the forces and that the mounting methods could be ignored. This needs to be tested with more rigor.

The second issue is the design for measuring RPM. The RPM input failed to provide adequate data on engine RPM and RPM had to be estimated from the forces. This was

not always possible, especially in data sets that have multiple peaks that show the same 2:3 relationship of propeller forces to engine power strokes. A root cause analysis needs to be performed on the RPM sensor circuit and a robust method needs to be devised before continuing with the data collection effort.

Chapter 7 Future Work

I would like to make three modifications to the system, probably in two phases. This first phase would be to fix or replace the RPM input circuit with a circuit that is more reliable, and to develop a method of measuring the force required to move the engine in its mounts. With these modifications, it will be possible to gain additional accuracy in the force measurements.

In the second phase I would replace the signal conditioning box and laptop with a smaller, DC powered device that would allow the measurement system to measure forces in flight. This will require the recording device to be able to handle large serial flash drives as a typical flight is a minimum of 15 to 20 minutes from engine start to shutdown with most lasting up to 3 hours. A flight of three hours requires a flash drive of at least 256 Mbytes as follows:

$$16\frac{Channel}{Sample} * 2\frac{Bytes}{Channel} = 32\frac{Bytes}{Sample} * 512\frac{Sample}{Sec} = 16{,}384\frac{Bytes}{Second}$$

$$16{,}384\frac{Bytes}{Second} * 3600\frac{Second}{Hour} \approx 59\frac{Mbytes}{Hour} * 3Hours \approx 177Mbytes$$

The nearest removable flash drive that is larger than this figure is 256 Mbyte. The basic requirements for the recorder would be the same as those contained in Chapter 3 with the following additional requirements:

- small size,
- the ability to record directly to a flash drive,
- be 12V DC powered,
- use removable flash, and
- be able to withstand maneuvering forces.

This system would be the next generation acquisition system that would provide information on the actual forces experienced in flight.

REFERENCES

1. http://imu.ieee-ims.org/school.php February 12, 2008
2. http://zone.ni.com/devzone/cda/tut/p/id/3642 February 13, 2008
3. http://zone.ni.com/devzone/cda/ph/p/id/12 February 13, 2008
4. http://www.memsic.com/products/technology.htm Feb 18, 2008
5. Ramon Pallàs-Areny and John G Webster,Sensors and Signal Conditioning, Second Edition, A Wiley-Interscience Publication, 2001, P4.
6. Drawing from Electronic Work Bench's Multisim V9
7. Analog Devices AD 522 Data Sheet
8. Linear Data Book 1980, National Semiconductor, p 4-19
9. John A. Camara PE, Electrical Engineering Reference Manual for the Electrical and computer PE Exam, Sixth Edition, Professional Publications Inc, Belmont, CA, 2002, p 44-5, figure b
10. http://www.allaboutcircuits.com/vol_2/chpt_8/2.html February 24, 2008
11. http://www.allaboutcircuits.com/vol_2/chpt_8/3.html February 24, 2008
12. http://www.allaboutcircuits.com/vol_2/chpt_8/4.html February 24, 2008
13. http://hyperphysics.phy-astr.gsu.edu/hbase/electronic/adc.html February 24, 2008
14. Private Pilot Manual, Jeppesen 8025 E 40th Avenue, Denver CO 80207 J4922B p 3-7\\
15. http://www.av8n.com/how/htm/yaw.html#8
16. http://home.hiwaay.net/~langford/corvair/flexplate/problem.html
17. http://home.hiwaay.net/~langford/corvair/index.html March 3,2008
18. http://home.hiwaay.net/~langford/corvair/index.html March 4, 2008
19. http://csep10.phys.utk.edu/astr161/lect/history/newtn3laws.html March 5, 2008
20. Alan V. Oppenheim, Alan S. Willsky with S. Hamid NAwab, "Signals and Systems Second Edition", 1997, p 519
21. Created by author using Microsoft Viso.
22. Created by Newest Computers Inc. Reno NV using OCAD V13
23. Created by ViewMate Gerber Viewer Software from CAD files developed by Newest Computers Inc.
24. Alan V. Oppenheim, Alan S. Willsky with S. Hamid NAwab, "Signals and Systems Second Edition", 1997, page 47
25. Plots created from analysis software created for this project by the author
26. Alan V. Oppenheim, Alan S. Willsky with S. Hamid NAwab, "Signals and Systems Second Edition", 1997, page 211
27. Alan V. Oppenheim, Alan S. Willsky with S. Hamid NAwab, "Signals and Systems Second Edition", 1997, page 212
28. Alan V. Oppenheim, Alan S. Willsky with S. Hamid NAwab, "Signals and Systems Second Edition", 1997, page 213
29. UNR Classroom assignment "Digital Signal Processing" EE 484, Spring 2005, Java class assignment, Professor Dr. James Henson.
30. Analysis using Microsoft Excel and rata from acquisition software.
31. Memsic sensor data sheet for +/. 5g accelerometer (MXR6150GM) http://www.memsic.com/memsic/data/products/MXR6150M/mxr6150gm.pdf (accessed Dec 14, 2007)

32. R.B. Randdall and B. Tech, B.A., Application of BK Equipment to Frequency Analysis, Second Edition, Naerom Offset Tryk, Naerum, Denmark, 1977, Ch 5
33. R.B. Randdall and B. Tech, B.A., Application of BK Equipment to Frequency Analysis, Second Edition, Naerom Offset Tryk, Naerum, Denmark, 1977, Ch 6

ATTACHMENT 1
Calibration Strip Charts

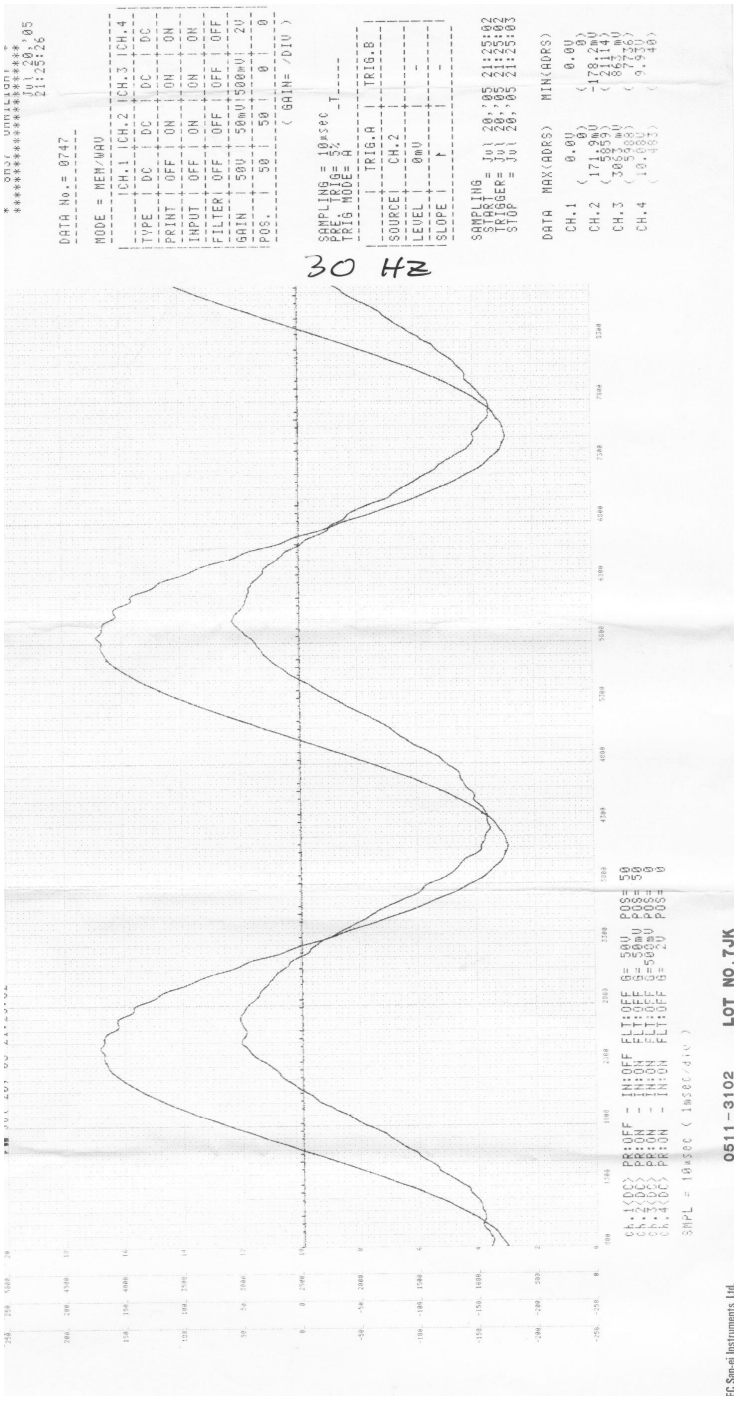

MODE:MEM/WAV Jul 20,'05 21:22:20 No.=0742

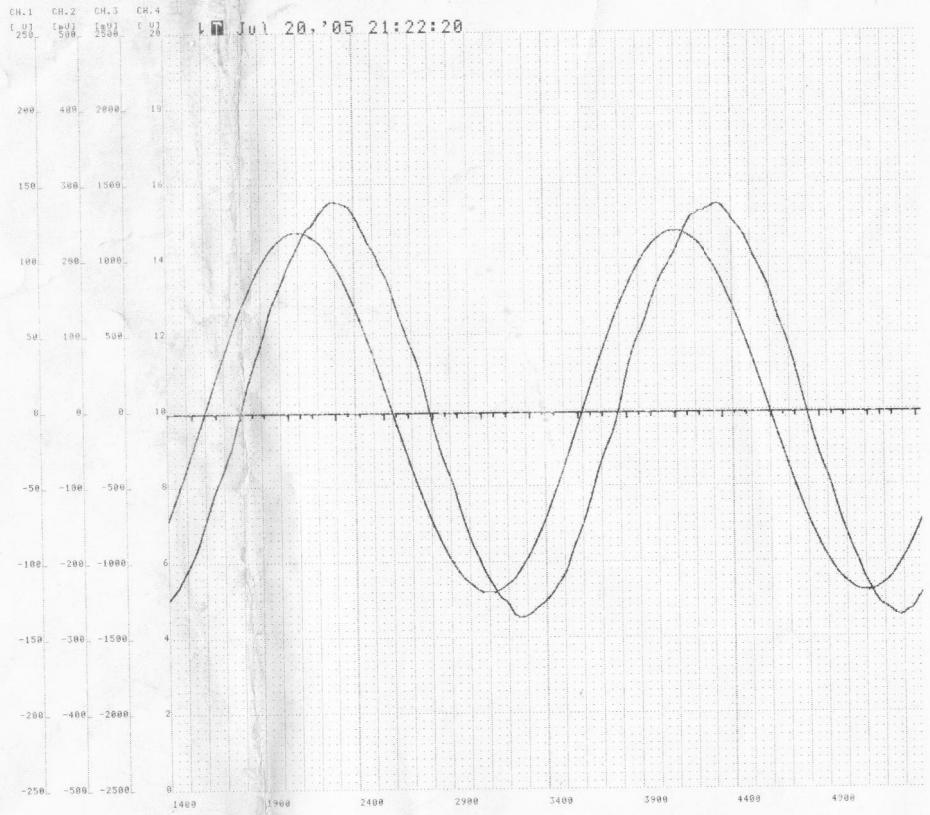

ch.1(DC) PR:OFF - IN:OFF FLT:OFF G= 50V POS= 50
ch.2(DC) PR:ON - IN:ON FLT:OFF G=100mV POS= 50
ch.3(DC) PR:ON - IN:ON FLT:OFF G=500mV POS= 50
ch.4(DC) PR:ON - IN:ON FLT:OFF G= 2V POS= 0

SMPL = 10μsec (1mSEC/div)

****
* 8M37 OMNILIGHT *
****
Jul 20,'05
21:22:36

DATA No.= 0742

MODE = MEM/WAV

	CH.1	CH.2	CH.3	CH.4
TYPE	DC	DC	DC	DC
PRINT	OFF	ON	ON	ON
INPUT	OFF	ON	ON	ON
FILTER	OFF	OFF	OFF	OFF
GAIN	50V	100mV	500mV	2V
POS.	50	50	50	0

(GAIN= /DIV)

SAMPLING = 10μsec
PRE. TRIG= 5%
TRIG MODE= A

	TRIG.A	TRIG.B
SOURCE	CH.2	
LEVEL	0mV	-
SLOPE	↑	-

SAMPLING
START = Jul 20,'05 21:22:20
TRIGGER= Jul 20,'05 21:22:20
STOP = Jul 20,'05 21:22:20

DATA	MAX(ADRS)	MIN(ADRS)
CH.1	0.0V (0)	0.0V (0)
CH.2	238 mV (12105)	-242 mV (1083)
CH.3	1382 mV (286)	-1400 mV (21288)
CH.4	9.96V (35)	0.00V (0)

52 42

NEC San-ei Instruments, Ltd. 0511-3102 LOT NO.7JK

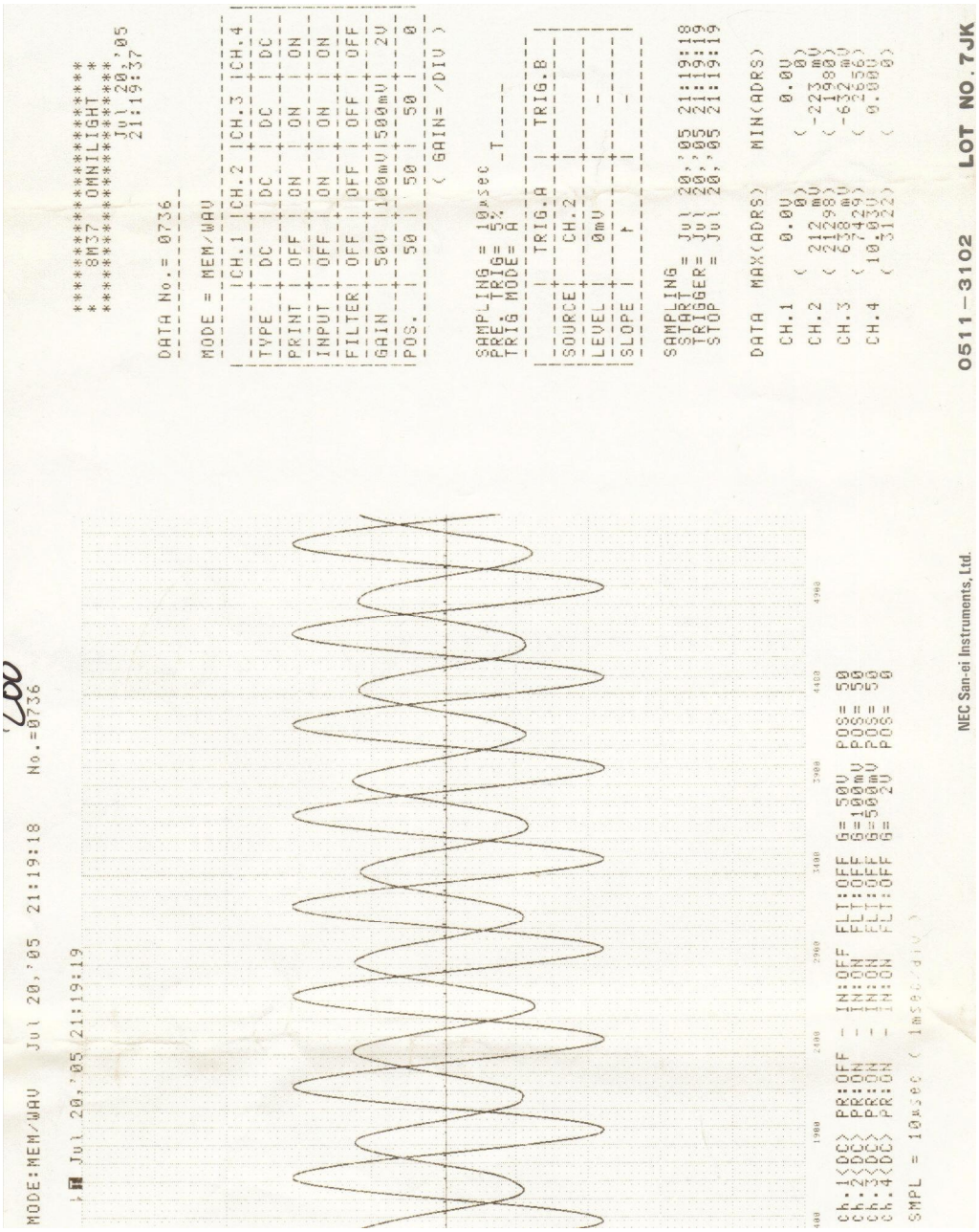
MODE:MEM/WAV Jul 20,'05 21:19:18 No.=0736
Jul 20,'05 21:19:19
ch.1<DC> BR:OFF - IN:OFF FLT:OFF G= 50V POS= 50
ch.2<DC> BR:ON - IN:ON FLT:OFF G=100mV POS= 50
ch.3<DC> BR:ON - IN:ON FLT:OFF G=500mV POS= 50
ch.4<DC> BR:ON - IN:ON FLT:OFF G= 2V POS= 0
SMPL = 10μsec (1msec/div)
********** 8M37 OMNILIGHT **********
Jul 20,'05 21:19:37
DATA No.= 0736
MODE = MEM/WAV
ICH.1 ICH.2 ICH.3 ICH.4
TYPE DC DC DC DC
PRINT OFF ON ON ON
INPUT OFF ON ON ON
FILTER OFF OFF OFF OFF
GAIN 50V 100mV 500mV 2V
POS. 50 50 50 0
(GAIN= /DIV)
SAMPLING = 10μsec
PRE. TRIG= 5%
TRIG MODE= A
TRIG.A TRIG.B
SOURCE CH.2
LEVEL 0mV
SLOPE
SAMPLING
START = Jul 20,'05 21:19:18
TRIGGER= Jul 20,'05 21:19:19
STOP = Jul 20,'05 21:19:19
DATA MAX(ADRS) MIN(ADRS)
CH.1 0.0V 0.0V
(0) (0)
CH.2 (212mV) (-223mV)
(212998) (-19980)
CH.3 (638mV) (-632mV)
(7429) (-2656)
CH.4 (10.03V) (9.00V)
(3122) (0)
NEC San-ei Instruments, Ltd.
0511-3102 LOT NO.7JK

Appendix 2

Dan Benson's Engineering Analysis
PROPELLER STRESSES ON CORVAIR CRANKSHAFT –Rev1
25March03

Introduction:

Moving a propeller further forward in an aircraft enhances propeller efficiency, streamlining, and esthetics. An extension of the propeller increases the loads and stresses in the engine crankshaft. This paper quantifies the effects of prop extension on a Corvair conversion. The aircraft studied is a Pietenpol with wood prop.

Part 1: Loads on the Crankshaft

Thrust. Thrust produces a tension load parallel to the crank
Torque. Torque produces a shear load
Weight. The weight of the propeller and the ring gear produce bending and shear stresses.
Precession. Precession is a bending load that results from gyroscopic characteristics of a rotating propeller and ring gear resisting flight maneuvers.

Load Evaluation:

M_t = Propeller Shaft Torque, in-lb
W_p = Propeller Weight, lb (10 lb, 62" dia)
W_{fw} = Flywheel Weight, lb (6 lb , 10" dia)
n = Flight Load Factor, g's = 2.5 per FARs
T = Propeller Thrust, lb = max per FARs
ω_y = Yaw Angular Rate = 2.5 rads/sec per FARs
ω_p = Pitch Angular Rate = 1 rads/sec per FARs

Thrust. The Corvair engine makes 90 hp at 3000 rpm. The relationship between **T**hrust, horse**P**ower, and **V**elocity is:

$$T = P/V$$
$$T = (90 \times 33000 /60) / 88 = \underline{\mathbf{562}} \text{ lb}$$

Torque. Computation of the mean torque of the Corvair at 90 hp and 3000 rpm produces:

$$M_t = (63000xP)/N = (63000x90)/3000 = \mathbf{1890} \text{ in-lb}$$

Applied at 75% of blade span yields:

$$F_t = (1890/2)/23.25 = \underline{\mathbf{81.3}}\# \text{ (up on LH side, down on RH side)}$$

Weight. Assume the prop weighs 10 lb and the ring gear weighs 6 lb. Per FAR's the load factor is 2.5 g's:

$$W_p' = W_p \times n = 10 \times 2.5 = \underline{\mathbf{25}}\text{lb}$$
$$W_{fw}' = W_{fw} \times n = 6 \times 2.5 = \underline{\mathbf{15}}\text{lb}$$

Precession. Gyroscopes want to maintain their plane of rotation. When one tilts a gyroscope, a moment 90° to the direction of tilt is generated – precession.

J_m = mass moment of inertia, prop or flywheel

ω_p = Engine RPM, rads/sec

ω_n= aircraft net maneuver rotational speed, rads/sec

g = gravitational constant 386 in/sec^2

The moment from precession is computed via…

$$M_{pp} = J_m \times \omega_p \times \omega_n \quad [1]$$

To calculate J_m of the propeller, it is represented by a bar. Then

$$J_m = ml^2/12 = (w_p/g)\, l^2/12 = (10/386)\, 62^2/12 = \mathbf{8.3} \text{ in-lb/sec}^2$$

And

$$\omega_p = 3000 \text{ rpm} \times 2\pi \text{ rads/rev} \times \text{min/60sec} = \mathbf{157}\text{rads/sec}$$

To calculate ω_n the vector summation of the yaw and pitch yielding.

$$\omega_n = (\omega_y^2+\omega_p^2)^{1/2} = (2.5^2+1^2)^{1/2} = \mathbf{2.69} \text{ rads/sec}$$

Inserting the rotational speeds into equation [1] yields:

$$M_{pp} = J_m \times \omega_p \times \omega_a = 8.3 \times 157 \times 2.69 = \underline{\mathbf{3505}} \text{ in-lb}$$

For the flywheel,

$$J_m = mr^2/2 = (W_{fw}/g)\, r^2/2 = (6/386)\, 5^2/2 = \mathbf{.0323} \text{ in-lb/sec}^2$$

Substituting into [1] gives:

$$M_{fw} = J_{fw} \times \omega_p \times \omega_g = .0323 \times 157 \times 2.69 = \underline{\mathbf{13.7}} \text{ in-lb}$$

Applied at 75% of a propeller blade span yields

$$T_{LH} = -(3505 + 13.7)/2 \,/\, 23.25 = \underline{\mathbf{-75.7}} \#$$
$$T_{RH} = (3505 + 13.7)/2 \,/\, 23.25 = \underline{\mathbf{75.7}} \#$$

Load Summary @ 75% Blade Span

Thrust = 281# axial

Torque = ±40.64# vert
Propeller Weight = 12.5# vertically downward
Flywheel Weight = 7.5# vertically downward
Precession = 75.7# axially backwards one blade, 75.7# forward other blade. These are applied conservatively to the model.

Viewed from the cockpit, and the CCW turning Corvair propeller:

RH yaw induces nose up precession
LH yaw drives the nose down.
Nose-up pitch results in LH precession.
Nose-down pitch results in RH precession.

Part 2: Analysis

Methods. The crankshaft was modeled in 3D in *SOLID WORKS*. The model was transferred to a finite element program, *COSMOS*. Two models were made: a crank with a William Wynne hub, and another with a 4" longer hub.

Restraints. Restraints are depicted in Figure 1. All four main journals were radial restrained at their axial centers. The end journal (distributor end) was additionally restrained in the axial and circumferential directions to react thrust and torque loads respectively. One case was run with the thrust restraint on the propeller end.

Load Cases. A dummy propeller was included in the model. The loads were resolved at the tips of the dummy propeller. The following load cases were applied:

a. WW hub at V_a and 1g. (Baseline)
b. WW hub at V_a w/ precession and 2.5 g's
c. 4" hub extension at V_a w/ precession and 2.5 g's

Part 3: Results

Results. Three stress runs were made. Von Mises stresses. COSMOS generates stress intensity in colors. The maximum stress occurred at the fictional junction of the dummy propeller and crankshaft which is not of interest.
a. WW hub: 5000 psi at 1st throw pin
b. WW hub Manuevering : 8900 psi @ shaft/cheek interface
c. 4" Extended Hub Manuvering: 9000 psi @ shaft/cheek interface

Discussion.

From this analysis, the loads imposed by maneuvering flight do not appreciable increase the stresses in the crankshaft with the WW hub or a 4" extended hub. The approximate endurance limit for the crankshaft material is 35000psi, the maximum applied load was 9000 psi.

THANKS,
Special thanks to Michael Piecyk who constructed the SOLID WORKS model and ran the COSMOS analysis – more than once

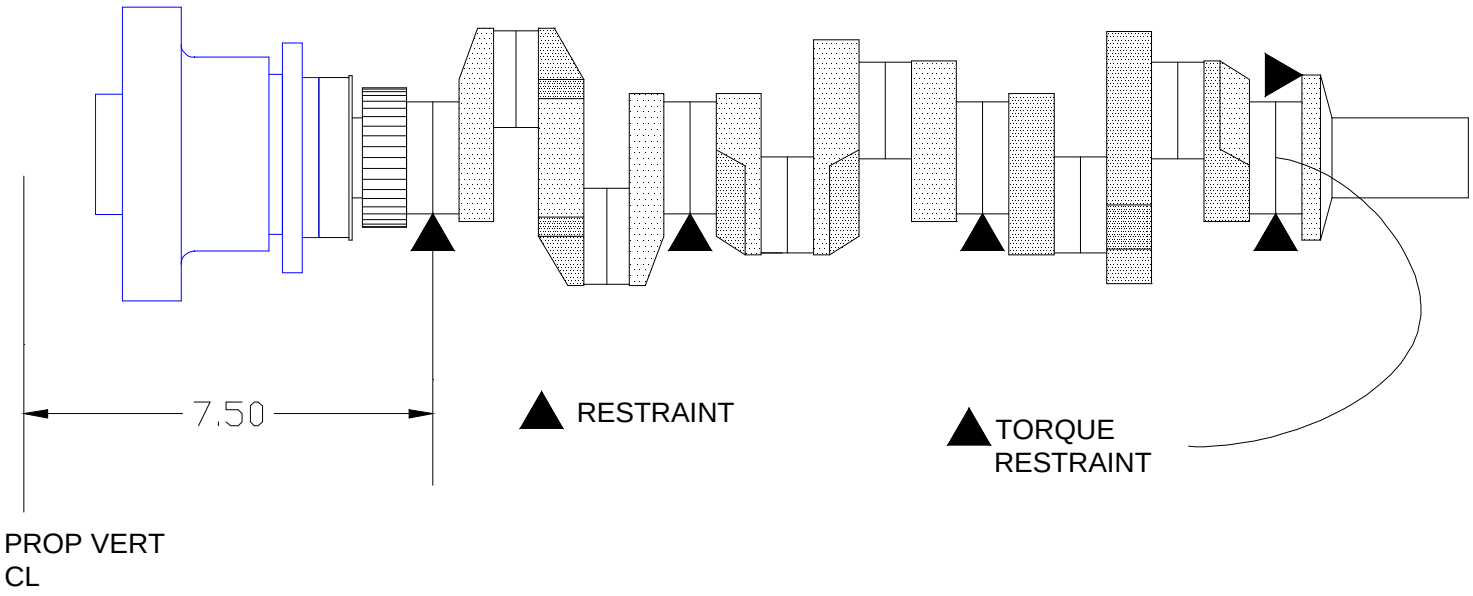

FIG 1: CRANK RESTRAINTS

Appendix 3

Memsic Application Note AN00MX-003

http://www.memsic.com/data/pdfs/an-00mx-003.pdf

Application Note
#AN-00MX-003

Thermal Accelerometers Frequency Compensation

Introduction

The response of each family of thermal accelerometers is a function of the internal gas physical properties and the sensor electronics. Since the gas properties of MEMSIC's mass produced accelerometers are uniform, a circuit like the one shown below can be tuned to compensate all sensors in a given accelerometer family. For most applications the compensating circuit does not require adjustment for individual units.

The frequency response of the standard MEMSIC thermal accelerometers is characterized by a –3dB point above 30Hz. A simple circuit is presented here to enhance the frequency response of the absolute analog output accelerometer type, operating at 5V supply. The network described below extends the –3dB point to well beyond 160 Hertz.

Accelerometer Frequency Response

The characteristic accelerometer amplitude frequency response has the form:

$$\sqrt{\frac{1}{\left[1+\left(\frac{f}{f1}\right)^2\right]\cdot\left[1+\left(\frac{f}{f2}\right)^2\right]\cdot\left[1+\left(\frac{f}{f3}\right)^2\right]}}$$

where f_1 is the convection system frequency response and is approximately 40 Hz, f_2 is the internal temperature sensor frequency response and it is approximately 85Hz and f_3 is the internal filtering circuit frequency response and it is above 300Hz.

Compensating Network

A simple compensating network comprising two operational amplifiers and a few resistors and capacitors provides increasing gain with increasing frequency (reference Figure 1).

The 14.3KΩ and the 5.9KΩ resistors along with the non-polarized 0.82μF capacitors tune the gain of the network to compensate for the output attenuation at the higher frequencies. The other resistors and capacitors provide noise reduction and stability.

The circuit has a DC gain of two, doubling the zero g offset as well as the sensitivity.

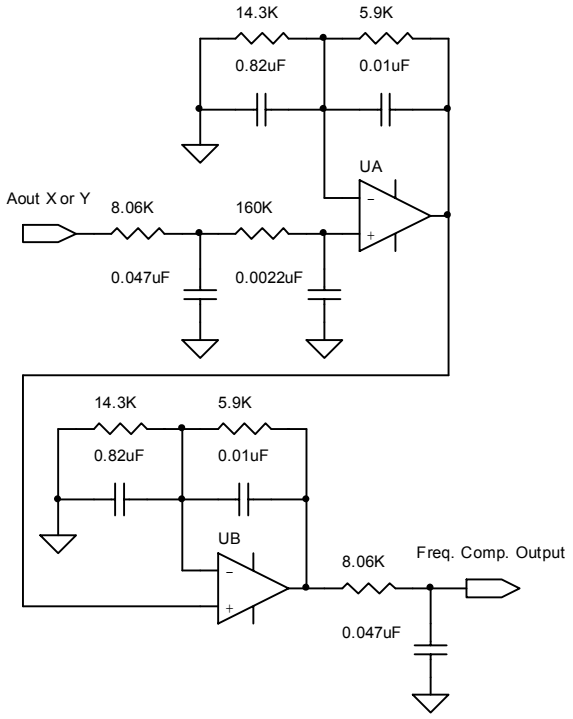

Figure 1: Frequency Enhancement Network

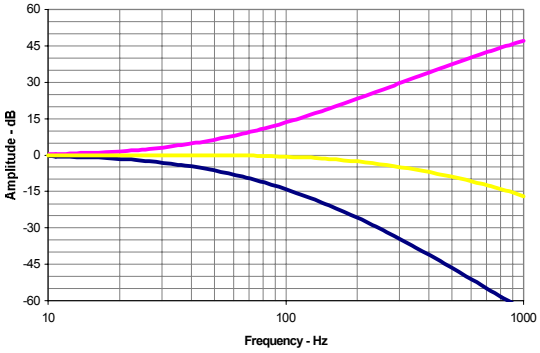

Figure 2: Amplitude Frequency Response

Compensated Response

The accelerometer response (bottom trace), the network response (top trace) and the compensated response (middle trace) are shown in Figure 2. The amplitude remains above –3db to 160 Hertz, and there is useable signal well beyond this frequency.

Conclusion

MEMSIC's thermal accelerometer technology may be applied to control systems, motion detection and inertial measurement applications when frequency response in hundred's of Hertz is required.